Aus der Medizinischen Klinik mit Schwerpunkt Nephrologie und
internistische Intensivmedizin der Medizinischen Fakultät
der Charité–Universitätsmedizin Berlin

DISSERTATION

Funktionelle Charakterisierung der endothelvermittelten autoimmunen PAR-2 Aktivierung

Functional characterization of endothelial autoimmune PAR-2 activation

zur Erlangung des akademischen Grades
Doctor rerum medicinalium (Dr. rer. medic.)

vorgelegt der Medizinischen Fakultät
Charité – Universitätsmedizin Berlin

von

Lei Chen
aus Guangdong, China

Datum der Promotion

21.06.2020

Table of contents

Abbreviations

AECA	Antiendothelial cell antibodies
Ang II	Angiotensin II
AR	Adrenergic receptor
AT_1R	Angiotensin II type 1 receptor
B2M	Beta-2 microglobulin
bp	Base pair
cAMP	Cyclic adenosine monophosphate
cDNA	Complementary DNA
Conc.	concentration
DNA	Deoxyribonucleic acid
EC	Endothelial cells
ECL	Extracellular loop
ECM	Extracellular matrix
EGF	Epidermal growth factor
ERK1/2	Extracellular signal-regulated kinases 1 and 2
FGF	Fibroblast growth factor
GAPDH	Glyceraldehyde 3-phosphate dehydrogenase
GFP	Green fluorescent protein
GPCR	G protein-coupled receptor
HIF1 α	Hypoxia induced factor 1 alpha
HIF2 α	Hypoxia induced factor 1 alpha
HMEC-1	Human microvascular endothelial cells
HUVEC	Human umbilical vein endothelial cells
ICL	Intracellular loop
IgG	Immunoglobulin class G
IL-6	Interleukin 6

IL-8	Interleukin 8
JNK	c-Jun kinase
kD	Kilodalton
LB	Lysogeny broth
M	Molar
mAchR	Muscarinic acetylcholine receptor
MAPK	Mitogen-activated protein kinase
miRNA	MicroRNA
mL	Milliliter
mRNA	Messenger RNA
NFAT	Nuclear factor of activated T-cells
nm	Nanometer
PAR-1	Protease-activated receptor 1
PAR-2	Protease-activated receptor 2
PAR-2-IgG	IgG targeting PAR-2
PAR-2 AP	PAR-2 activating peptide
PAR-3	Protease-activated receptor 3
PAR-4	Protease-activated receptor 4
PBS	Dulbecco’s phosphate buffered saline
PCR	Polymerase chain reaction
PKC	Protein kinase C
qRT-PCR	quantitative Real Time-PCR
RhoA	Rho guanine nucleotide exchange factors
RNA	Ribonucleic acid
ROCK	Rho-associated protein kinase
SD	Standard deviation
SEM	Standard error of the mean
SRE	Serum response element

SRF	Serum response factor
SSc	Systemic sclerosis
STAT3	Signal transducer and activator of transcription 3
TGF-β	Tissue growth factor beta
TNF-α	Tumor necrosis factor alpha
TSH	Thyrotropin, thyroid stimulating hormone
TSHR	Thyroid stimulating hormone receptor
VEGF	Vascular Endothelial Growth Factor
VEGFR	Vascular endothelial growth factor receptor
α1 AR	α1-adrenergic receptor
β1 AR	β1-adrenergic receptor
β2 AR	β2-adrenergic receptor
µg	Microgram
µL	Microliter

List of tables

List of figures

Abstract

Background:

Protease-activated receptor 2 (PAR-2) is a G protein-coupled receptor (GPCR) involved in angiogenesis. Autoantibodies targeting certain membrane receptors can influence angiogenesis and cancer development after transplantation. The presence of autoantibodies directed against PAR-2 (PAR-2^{+}-IgG) in kidney transplant (KTx) patients and its angiogenic function have not been studied so far.

Methods:

IgGs were isolated from serum of healthy individuals and KTx patients by HiTrap Protein G columns and PAR-2 (PAR-2^{+}-IgG) levels were confirmed by ELISA. PAR-2 signaling in response to natural activator trypsin, PAR-2 activating peptide (PAR-2 AP) and PAR-2^{+}-IgG was studied in wild-type and PAR-2 overexpressing HMEC-1 by western blots and luciferase reporter assays. Real time PCR and ELISA were performed to study the effect of PAR-2 agonists and IgG on VEGFA production. The effect of PAR-2^{+}-IgG on angiogenesis was studied using matrigel angiogenesis assay with endothelial cells.

Results:

PAR-2 levels from KTx patients (PAR-2^{-}-IgG) were lower than those from healthy controls (PAR-2^{+}-IgG). Trypsin and PAR-2 AP activated $G_{\alpha 12/13}$, G_{q11} and ERK1/2 signaling in PAR-2 overexpressing HMEC-1 cells in a dose-dependent manner. This resulted in increased promotor activity, mRNA and protein levels of VEGFA. PAR-2^{+}-IgG activated $G_{\alpha 12/13}$, G_{q11} and ERK significantly more strongly than PAR-2^{-}-IgG. PAR-2^{+}-IgG increased VEGFA at both mRNA and protein level, which could be partially blocked by a PAR-2 specific blocker. Angiogenesis assay showed that PAR-2^{-}-IgG reduced vascular endothelial tube formation.

Conclusion:

The results here confirmed that PAR-2 couples with multiple G proteins, including $G_{\alpha 12/13}$ and G_{q11}, activates ERK, and leads to increased VEGFA in endothelial cells by the natural activator trypsin. PAR-2 autoantibodies present in healthy individuals activated same signaling cascades as trypsin and PAR-2 AP and were proangiogenic. In contrast, PAR-2^{-}-IgG from KTx patients were anti-angiogenic. The clinical relevance of this reduced *in vitro* angiogenesis of PAR-2^{-}-IgG from KTx

patients has to be investigated in larger cohort studies in the future. It will be of interest whether these low PAR-2 antibody levels can be used as biomarkers, e.g. for cancer development, as demonstrated for PAR-1 autoantibodies.

Abstrakt

Hintergrund:

Protease-aktivierter Rezeptor 2 (PAR-2) ist ein G Protein gekoppelter Rezeptor (GPCR), der bei Angiogenese eine wichtige Rolle spielt. Autoantikörper, die gegen bestimmte Membranrezeptoren gerichtet sind, können Angiogenese und auch die Entwicklung von Krebs nach Transplantation beeinflussen. Das Vorkommen von Autoantikörpern gegen PAR-2 bei Nierentransplantationspatienten (KTx) und deren potentiell proangiogene Funktion wurden bislang noch nicht untersucht.

Methoden:

Mittels HiTrap Protein G Säulen wurde IgG aus dem Serum von gesunden Kontrollpersonen und nierentransplanierten Patienten isoliert und PAR-2 Autoantikörpertiter durch ELISA bestimmt. In Wildtyp und PAR-2 überexprimierenden HMEC-1 wurden PAR-2 abhängige Signalwege nach Aktivierung durch Trypsin, PAR-2 aktivierendes Peptid (PAR-2 AP) und PAR-2^{+}-IgG wurden mittels Westernblots und Luziferase Reporter Assays untersucht. Real time PCR und ELISA wurden verwendet, um die Effekte der PAR-2 Agonisten und IgG auf die VEGF Freisetzung zu bestimmen. Der Einfluss von PAR-2^{+}-IgG auf die Angiogenese wurde durch Matrigel-Angiogeneseassays mit Endothelzellen analysiert.

Ergebnisse:

PAR-2 Autoantikörpertiter von nierentransplantierten (PAR-2^{-}-IgG) Patienten waren niedriger als in gesunden Kontrollen. In PAR-2 überexprimierenden HMEC-1 wurde durch Trypsin und PAR-2 AP der $G_{\alpha 12/13}$-, G_{q11}- und ERK1/2-Signalweg konzentrationsabhängig aktiviert. Dies führte zu einer erhöhten Promotoraktiviät, mRNA- und Proteinspiegel von VEGFA. PAR-2^{+}-IgG aktivierte den $G_{\alpha 12/13}$-, G_{q11}- und ERK1/2-Signalweg signifikant stärker als PAR-2^{-}-IgG. PAR-2^{+}-IgG erhöhte VEGFA sowohl auf mRNA, als auch auf Proteinebe, welches partiell durch PAR-2 spezifische Blocker gehemmt werden konnte. Angiogenesisassays zeigten, dass PAR-2^{-}-IgG zu einer verminderten endothelialen Netzwerkbildung führt.

Schlussfolgerung:

Die Ergebnisse dieser Arbeit bestätigen, dass PAR-2 an mehrere G Proteine koppelt, darunter $G_{\alpha 12/13}$ und G_{q11}, den ERK-Signalweg aktiviert und zu erhöhtem VEGFA in Endothelzellen durch

natürlichen Aktivator Trypsin führt. PAR-2 Autoantikörper von gesunden Personen aktivierten die gleichen Signalkaskaden wie Trypsin und PAR-2-AP und waren proangiogen. Dagegen wirkten PAR-2$^-$-IgG von KTx Patienten antiangiogen. Die klinische Bedeutung dieser verminderten *in vitro* Angiogenese von PAR-2$^-$-IgG von KTx Patienten sollte in zukünftigen größeren Kohortenstudien untersucht werden. Es wäre interessant, inwieweit niedrige PAR-2-Antikörperspiegel z.B. analog zu PAR-1 Autoantikörperspiegeln als Biomarker für ein erhöhtes Krebsrisiko eingesetzt werden könnten.

1 Introduction

1.1 Clinical background

Kidney transplantation is considered to be the optimal therapy for patients with end-stage renal disease (ESKD).(1) After kidney transplantation, antibody-mediated rejection and increased incidence of cancer affect the life span and quality of life of the recipients.(2, 3) Autoantibody-mediated receptor activation has been recognized as a factor that contributes to various diseases.(4) Stimulatory autoantibodies that recognize the angiotensin II type 1 receptor (AT_1R) can lead to severe vascular rejection in kidney transplant recipients.(5) Autoantibodies against protease-activated receptor 1 (PAR-1) in kidney transplant recipients negatively correlated with the development of metastatic cancer and the survival of those patients post renal transplantation due to the anti-angiogenic effect of those autoantibodies.(6) The presence of autoantibodies directed against another membrane receptor, protease-activated receptor 2 (PAR-2) has never been reported before, and their functions remain unexplored. Angiogenesis is known to contribute to the development of various complications after transplantation. Thus, this thesis is focused on the investigation of the potential proangiogenic effect of autoantibodies directed against PAR-2, extending current knowledge about PARs in proangiogenic pathomechanisms.

1.2 PAR-2

1.2.1 PAR-2, receptor of proteases

PAR-1 and PAR-2 are members of the protease-activated receptors (PARs) family, which currently comprises four members, namely PAR-1, PAR-2, PAR-3 and PAR-4.(7) PAR-2, also known as coagulation factor II receptor-like 1, G-protein coupled receptor 11, or thrombin receptor-like 1, is the second member of the PARs family. Natural PAR-2 agonists include trypsin, tryptase, Factor VIIa and Factor Xa.(7)

1.2.2 PAR-2 gene and protein

The human PAR-2 gene is located in chromosome region 5q13 near the PAR-1 gene, and consists of 2 exons.(8) The PAR-2 protein contains 687 amino acids, with a molecular mass predicted to

be about 44kDa. Human PAR-2 is glycosylated on two N-linked glycosylation sites located at Asn30 within the N-terminus, and at Asn222 within extracellular loop 2 (ECL2).(9) N-linked glycosylation not only facilitates cell surface expression of the receptor, but also affects receptor signaling.(9)

PAR-2 displays a wide tissue and cell expression pattern. It is abundantly distributed in skin, lung, brain, prostate, vasculature, colon and uterus.(10) It is highly expressed in vascular endothelial cells (EC), epithelial cells, neuronal cells, keratinocytes and fibroblast cells.(10)

1.2.3 PAR-2 activating mechanism

Proteases activate PAR-2 via a unique mechanism of proteolysis. The protease cleaves the receptor after recognizing a specific enzymatic site located at the extracellular N-terminus, $SKGR^{34}\downarrow S^{35}LIGKV$ in humans.(11) This irreversible cleavage generates a new N-terminus that in turn serves as a tethered ligand, binding to the extracellular domain of the same receptor and initiating receptor activation.(11) (Figure 1) Furthermore, receptor site-directed mutation experiments revealed that amino acids within ECL2 (residues Val212–Leu235) are essential for tethered ligand-mediated receptor activation.(12)

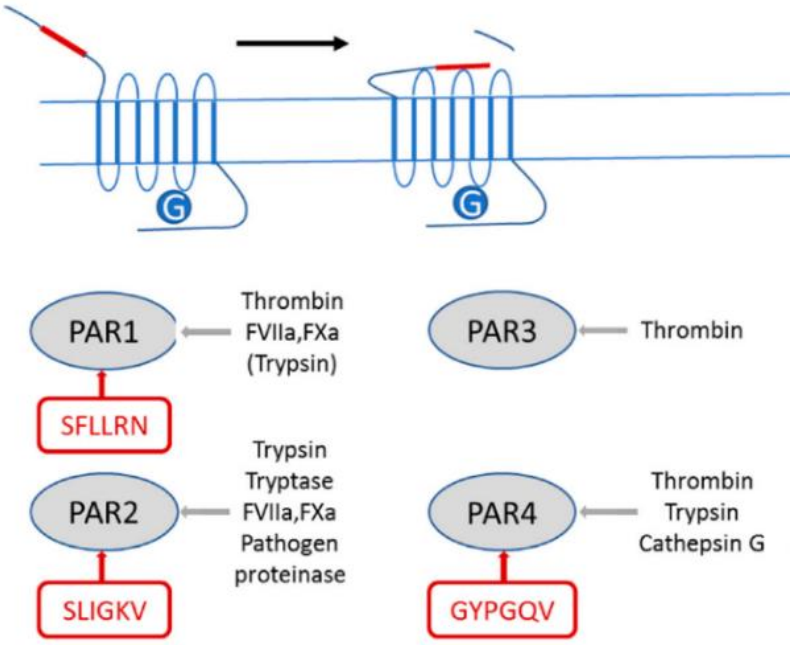

Figure 1. Mechanism of PARs activation and their agonists. (13)

1.2.4 PAR-2 cellular signaling pathways

Compared with PAR-1, the signaling mechanism of PAR-2 is still largely unknown. However, there are several lines of evidence suggesting that PAR-2, like other GPCRs, couples with various G proteins and β-arrestins.(14, 15) PAR-2 couples to $G_{q/11}$ and $G_{\alpha 12/13}$ in COS-7 cells.(14) PAR-2 activation triggers the coupling of $G_{\alpha 12}$ and β-arrestin 1.(15) Both β-arrestin 1 and 2 are critical for the desensitization and internalization of PAR-2 after receptor activation.(16)

The cellular events upon PAR-2 activation include cell proliferation, migration, survival and release of multiple cytokines.(17) These events are mediated by the activation of multiple downstream signaling pathways.(Figure 2) Stimulated PAR-2 can activate multiple mitogen-activated protein kinase (MAPKs) signaling pathways, including extracellular signal-regulated kinase (ERK1/2), p38, and c-Jun NH2-terminal kinase (JNK).(18) Downstream of the phosphoinositide phospholipase C (PLC) activation, phosphorylation of IκB kinase-α (IKK-α) and IKK-β causes the activation and nuclear translocation of nuclear factor-kappa B (NF-κB), inducing the transcription of NF-κB dependent genes, such as intercellular adhesion molecule 1 (ICAM-1), interleukin 6 (IL-6), and interleukin 8 (IL-8).(18)

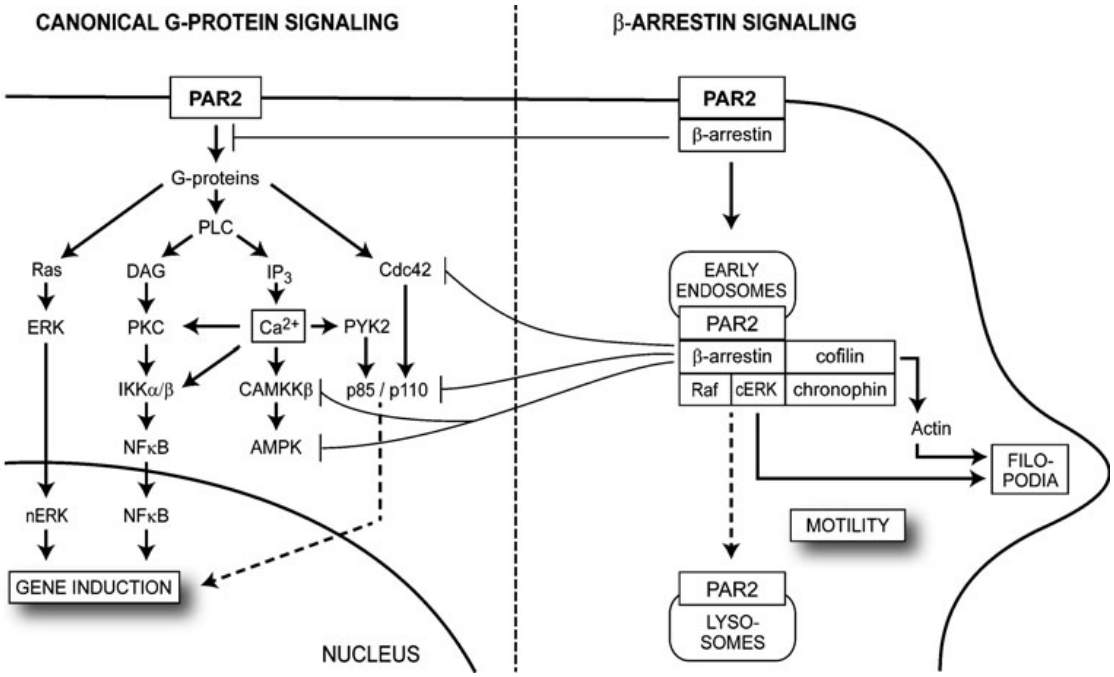

Figure 2. The canonical G-protein signaling and β-arrestin-dependent signaling induced by PAR-2 activation. (18)

1.2.5 PAR-2 in human pathology

PAR-2 modulates of a wide range of physiological and pathological processes. Abnormal PAR-2 levels have been related to the development and progression of various diseases, like cancer, atherosclerosis, IgA nephropathy, lung fibrosis, and cardiac hypertrophy.(19-23) Both PAR-2 mRNA and protein levels were elevated in biopsies from IgA nephropathy patients.(19) The protein level of PAR-2 and its ligand factor VIIa was elevated in idiopathic pulmonary fibrosis patients.(20) PAR-2 was essential for Factor VIIa and Xa–induced migration, and invasion of highly invasive breast cancer cells.(21) Systemic deletion or hematopoietic deletion of PAR-2 attenuated vascular inflammation and atherogenesis in the atherosclerotic mouse model.(22) In mice, overexpression of PAR-2 in cardiomyocyte led to heart hypertrophy, while cardiomyocyte-specific knockout of PAR-2 attenuated heart remodeling and improved heart function in a myocardial infarction model.(23)

1.3 Autoantibodies targeting GPCRs

1.3.1 Autoantibodies directed against GPCRs

Naturally occurring autoantibodies of the IgM, IgG and IgA classes, reactive with various serum proteins, cell surface structures and intracellular structures, have been identified in normal individuals.(24) Naturally occurring autoantibodies targeting G protein-coupled receptors (GPCRs) can also be detected in the serum of normal individuals, who never develop autoimmune disorders.(25) GPCRs, most of which signal via the interaction between intracellular domains and heterotrimeric G proteins, transduce multiple extracellular signals into intracellular signals, and regulate a wide range of physiological process.(26) If autoantibodies directed against GPCRs can agonize or antagonize the receptor after binding to the receptor, these autoantibodies will be of pathogenic and clinical significance. Indeed, autoantibodies directed against several GPCRs, including AT_1R, β1- and α1-adrenoceptor (β1 and α1 AR), and thyroid-stimulating hormone receptor (TSHR), have been characterized and related to diseases.(4) (Figure 3)

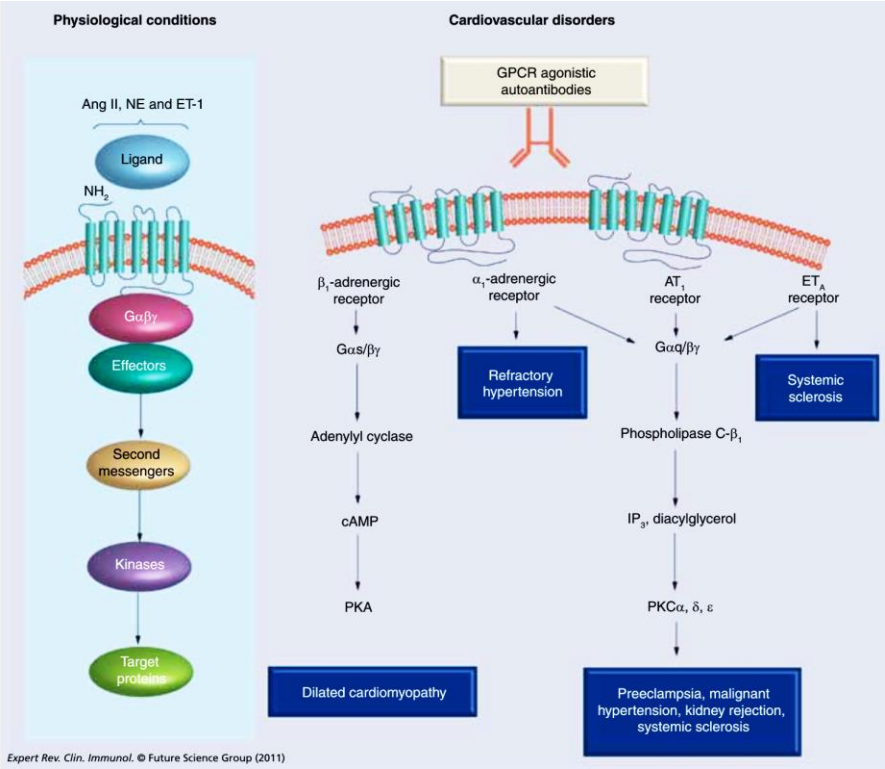

Figure 3. Contribution of cardiovascular receptor-agonistic autoantibodies to cardiovascular diseases. (4)

1.3.2 Autoantibodies targeting GPCRs in human pathology

Graves' patients have higher TSHR IgG levels compared to healthy controls. Mice injected with cDNA or adenoviruse encoding TSHR produced anti-TSHR autoantibodies and developed Graves'-like hyperthyroidism, proving the pathological role of TSHR autoantibodies in Graves' disease.(27, 28)

Autoantibodies directed against α1 AR and β1 AR are frequently present in serum from patients with hypertension and idiopathic dilated cardiomyopathy, respectively. β1 AR IgG recognizing the first or second ECL of the receptor activate the β1 AR signaling cascade, and its level is associated with cardiac function.(29) α1-AR IgG enhances the beating rate of neonatal rat cardiomyocytes.(30) Removal of α1-AR IgG by immune-adsorption could reduce blood pressure, suggesting the contribution of these autoantibodies to the development of refractory hypertension.(31)

AT_1R is the receptor for the small peptide Angiotensin II. AT_1R-agonistic, AT_1R IgG autoantibodies were initially demonstrated to contribute to the pathogenesis of preeclampsia.(32) Later, Dragun linked AT_1R IgG to the pathogenesis of vascular rejection.(5) AT_1R IgG present in

patients with systemic sclerosis (SSc) might contribute to the pathogenesis of SSc.(33)

1.4 VEGF: master regulator of angiogenesis

1.4.1 VEGF and angiogenesis

Angiogenesis, the sprouting of new capillaries from pre-existing blood vessels, is essential for vascular development and maintenance.(34) It occurs during diverse normal physiological processes, such as embryonic development, pregnancy, and wound healing.(34) Multiple growth factors, chemokines, cytokines and enzymes regulate angiogenesis directly or indirectly.(35) Vascular endothelial growth factor A (VEGFA) is considered to be a master regulator.

VEGFA is the key member of VEGF protein family which currently consists of five members, placental growth factor (PLGF), VEGFA, VEGFB, VEGFC and VEGFD. In heterozygous VEGF-deficient (*Vegfa*$^{+/-}$) embryos, blood vessel formation is impaired, but not abolished, and homozygous VEGFA-deficiency (*Vefga*$^{-/-}$) leads to embryonic lethality at mid-gestation due to significantly impaired vessel formation.(36) Adenoviral vector-mediated VEGFA delivery results in robust lymphangiogenesis and angiogenesis in mice *in vivo*.(37) In physiological processes, VEGFA signaling is a rate-limiting step and tightly controlled. The VEGFA level increases at the initiation step of angiogenesis, and declines at the resolution step of angiogenesis.(38)(Figure 4).

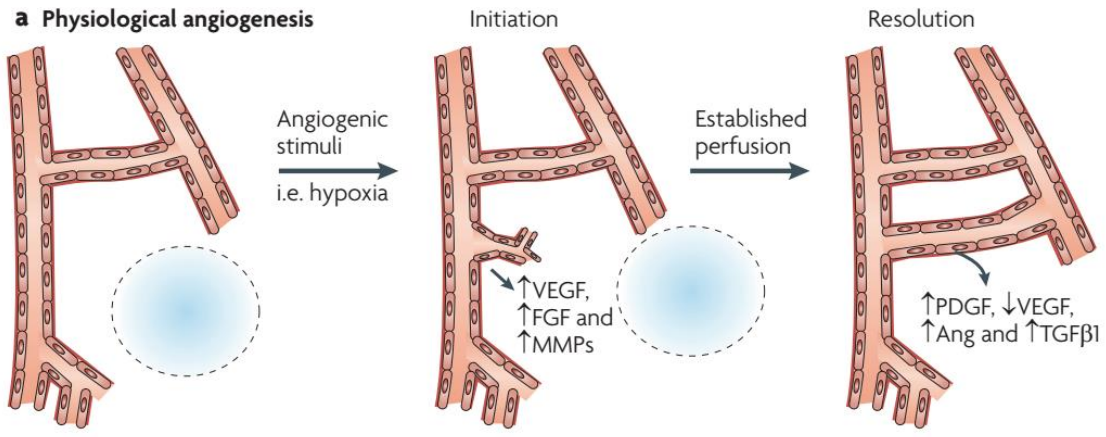

Figure 4. Physiological angiogenesis process. (38)

1.4.2 Regulation of VEGFA expression

Human *VEGFA* gene localizes to the chromosome 6p12 and is organized as eight exons.(39)

Alternative splicing of *VEGFA* mRNA, signal sequence cleavage, and proteolytic processing result in the generation of five major isoforms (VEGF121, VEGF145, VEGF165, VEGF189, and VEGF206), with VEGF165 being the most important isoform.(40)

Oxygen tension, growth factors and oncogenes are the main regulators of VEGF expression. Hypoxia induces *VEGFA* mRNA transcription via enhancement of hypoxia-inducible factor 1 α (HIF-1 α) binding to the hypoxia response element within the proximal promoter region.(41) Multiple growth factors, inflammatory cytokines and sex hormones, like TGF-β, IL-6, estrogen or androgen, can greatly induce VEGFA secretion.(42) Mutation of Ras oncogene or p53 tumor suppressor gene, or overexpression of SRC oncogene, can lead to abnormal VEGFA production.(43)

1.4.3 Physiological and pathological functions of VEGFA

The biological effects of VEGFA on endothelial cells are diverse. It is well-known that VEGFA can induce proliferation, sprouting, and migration of vascular EC derived from veins, arteries, and lymphatics *in vitro*.(43) VEGFA can also affect non-endothelial cells. VEGFA induces the activation and migration of human monocytes.(44) VEGFA exerts chemoattractive effect on human mesenchymal progenitor cells.(45) Cancer cell line-derived VEGFA inhibits the generation of dendritic cells from precursors, without any effect on relatively mature dendritic cells.(46)

Excessive or insufficient angiogenesis due to abnormal VEGFA signaling has been implicated in various pathologic conditions, including cancer, intraocular neovascular syndromes, and preeclampsia.(47-49) In preeclampsia patients, excess circulating placental soluble VEGFR-1 (sVEGFR-1) decreases levels of free VEGFA, resulting in endothelial dysfunction, hypertension, and proteinuria.(47) Hypoxia-induced VEGFA governs pathological retinal neovascularization and causes retinal neovascular diseases.(48) Inhibition of VEGF using soluble VEGFR chimeric proteins suppresses retinal neovascularization *in vivo*.(48) VEGFA is frequently upregulated in cancer patients.(49)Avastin®(bevacizumab), a humanized monoclonal antibody against VEGF, has been approved to treat various types of cancer.(49)

2 Hypothesis and Objectives

2.1 Hypothesis

Autoantibodies directed against various GPCRs have been detected in kidney transplant patients. These autoantibodies have been shown to influence renal function after transplantation by directly affecting endothelial cells. PAR-2 is a GPCR expressed in endothelial cells, whose activation influences inflammation, fibrosis and angiogenesis. Hence, it is hypothesized that kidney transplant patients present PAR-2 IgG, and that these IgG can activate PAR-2 and induce the expression of VEGF, thereby contributing to angiogenesis.

2.2 Objectives

In order to validate the hypothesis, it was necessary to clarify the intracellular signaling following PAR-2 activation, to investigate whether there are differences between kidney transplant patients and healthy individuals regarding PAR-2-IgG level and to assess the effects of PAR-2-IgG on VEGF and angiogenesis. Therefore, the objectives of this work were:

1. To quantify the level of PAR-2-IgG in healthy individuals and kidney transplant patients.
2. To establish a cell culture model in human microvascular endothelial cells 1 (HMEC-1) which allows the investigation of PAR-2 signaling.
3. To investigate G-protein signaling pathways activated by PAR-2, and to study the effect of PAR-2 activation on VEGF levels.
4. To characterize and compare G-protein signaling of PAR-2^{+}-IgG isolated from healthy individuals and kidney transplant patients.
5. To investigate the effect of PAR-2^{+}-IgG on VEGF expression in cultured HMEC-1 cells and on angiogenesis.

3 Materials and methods

3.1 Materials

3.1.1 Chemical substances

Reagents	Manufacturer
1 kb DNA ladder	NEB
10X Trypsin-EDTA	PAA
2-Propanol	Carl Roth
5X Passive Lysis Buffer (PLB)	Promega
50 bp DNA ladder	Thermo Fisher
Acrylamide (37.5:1) Rotiphorese® Gel 30	Carl Roth
Agarose	Carl Roth
Ampicillin	Alkom
BSA	Carl Roth
Chloroform	Carl Roth
Diethylpyro-carbonate (DEPC)	Sigma Aldrich
Dimethyl sulphoxide (DMSO)	Sigma Aldrich
Dithiothreitol (DTT)	AppliChem
DMEM Low glucose medium	Biowest
DNA Gel Loading Dye (6X)	Thermo Fisher
dNTP Mix	Thermo Fisher
Ethylenediamintetra-acetic acid (EDTA)	Carl Roth
ENMD-1068 hydrochloride	Sigma Aldrich
Ethanol 99.8%	Carl Roth
FastStart Universal SYBR Green Master (Rox)	Roche
Fetal Bovine Serum (FBS)	Gibco
Gelatine	Sigma
hEGF	Sigma Aldrich
Hydrocortisone	Sigma Aldrich

Reagents	Manufacturer
M-MuLV Reverse Transcriptase	NEB
Nonfat dried milk powder	AppliChem
NaF (Sodium Fluoride)	AppliChem
MCDB-131 medium	c.c.pro GmbH
Midori Green Direct	NIPPON Genetics Europe
MOPS	Applichem
PD 184352	Sigma Aldrich
Penicillin-Streptomycin Solution 100X	Biowest
Protease Inhibitor Tablets, Complete Mini	Roche Applied Science
Protein Marker VI (10-245) prestained	AppliChem
Ponceau S	Carl Roth
PVDF (polyvinylidene difluoride)	GE Healthcare
Oligo d(T)16 (50 µM)	Invitrogen
RNase inhibitor	ABI
Roche complete inhibitor	Roche Diagnostics GmbH
SB 203580	Calbiochem
Sodium azide	Sigma Aldrich
Sodium chloride	Carl Roth
Sodium hydroxide	Sigma Aldrich
Sodium orthovanadate (Na_3VO_4)	Roth
Sodium pyrophosphate	Applichem
Sodium dodecyl sulfat (SDS) Pellets	Carl Roth
SuperSignal West Pico	Thermo Scientific
SuperSignal West Dura	Thermo Scientific
Thrombin	Sigma Aldrich
Tri-Sodium citrate dihydrate	Carl Roth
Trypan blue	Sigma Aldrich
Trypsin-EDTA 10X	Biowest

Reagents	Manufacturer
Trypsin from bovine pancreas	Sigma Aldrich
Valsartan	Sigma Aldrich
WesternBright Sirius HRP substrate	Advansta

3.1.2 Antibodies

Antibodies	Company	dilution
Akt antibody (# 9272)	Cell signaling	1:1000
Alpha-Tubulin antibody	Sigma Aldrich	1:1000
GAPDH antibody (# 6C5CC)	HyTest	1:10000
p44/42 MAPK (Erk1/2) antibody (# 9102)	Cell signaling	1:1000
PAR-2 antibody (#sc-13504)	Santa Cruz	1:200
Peroxidase-conjugated AffiniPure Donkey Anti-Mouse IgG	Dianova	1:20000
Peroxidase-conjugated AffiniPure Donkey Anti-Rabbit IgG	Dianova	1:20000
Phospho-Akt (Ser473) antibody (# 9271)	Cell signaling	1:1000
Phospho-Akt (Thr308) antibody (# 9275)	Cell signaling	1:1000
Phospho-p38 MAPK antibody (#4511)	Cell signaling	1:1000
Phospho-p44/42 MAPK (Erk1/2) (Thr202/Tyr204) antibody (#9106)	Cell signaling	1:1000

3.1.3 Kits

Kit	Manufacturer
Buffer Kit for Antibody Pairs	Invitrogen
DC™ Protein Assay	Bio-Rad
Dual-Luciferase® Reporter Assay System.	Promega
GeneJET Plasmid Miniprep Kit	Thermo Fisher
Human VEGF Standard TMB ELISA Kit	PeproTech

Kit	Manufacturer
In-Fusion® HD Cloning Kit	Takara
Luciferase Assay System	Promega
NucleoBond®Xtra Midi/Maxi	MACHEREY-NAGEL
PeqGOLD MicroSpin Cycle pure Kit	VWR
Xfect Transfection Reagent	Takara

3.1.4 Equipment

Equipment	Manufacturer
Applied Biosystems® 7500 Real-Time PCR System	Thermo Fisher Scientific
Axiovert 40 CFL Microscope	Carl Zeiss
Digital Heatblock II	VWR
Duomax 1030 Platform Shaker	Heidolph Instruments
Electrophoresis Power Supply Model EPS-3500	Pharmacia Biotech
FLUOstar OPTIMA Microplate Reader	BMG LABTECH
FRESCO 21 Centrifuge	Thermo Electron Corporation
Gel documentation system, Syngene G:BOX Chemi XRQ	VWR
HERA cell 240 Incubator	Thermo Electron Corporation
HERA safe Microbiological Safety Cabinet	Thermo Electron Corporation
Heraeus / BB 6220 CU O_2	Thermo Fisher Scientific
Incubating Orbital Shaker professional 3500	VWR
Model 200/2.0 POWER SUPPLY	Bio-Rad
Multiskan Ascent 354 Microplate Reader	Thermo Fisher Scientific
ND-1000 Spectrophotometer	VWR
Rotor RS-TR05	Phoenix Instrument
SUB Waterbath	Grant
T Professional BASIC XL 96 Thermocycler	Biometra
UV-transilluminator Gene Flash	SYNGENE

3.1.5 Plasmids, bacteria, cell lines and enzymes

Plasmid	Company
pcDNA3.1^{+} vector	Invitrogen
pGL4.33[luc2P/SRE/Hygro] vector	Promega
pGL4.34[luc2P/SRF-RE/Hygro] vector	Promega
pGL4.30[luc2P/NFAT-RE/Hygro] vector	Promega
pRL Renilla Luciferase Control Reporter Vector	Promega

Cells	Company
Stellar™ Competent Cells	Clontech
Human Microvascular Endothelial Cells (HMEC-1)	Kindly provided by Dr. Orzechowski

Enzyme	Company
*BamH*I-HF	NEB
*EcoR*I-HF	NEB
*Hin*dIII-HF	NEB
*Xho*I	NEB

3.1.6 Buffers

Buffer	Reagent	Final Conc.
Blocking buffer (WB)	Nonfat dried milk powder	5% m/v
	BSA	1% m/v
	add 1x TBS-T	
Blocking buffer (ELISA)	1% BSA	1%
	add 1x PBS	
	Na_2HPO_4	0.02 mol/L

Buffer	Reagent	Final Conc.
	sterile by filter	
BICIN transfer buffer 1x	BICIN	25 mM
	Bis-Tris	25 mM
	EDTA, pH 8.0	1 mM
	Ethanol	10% v/v
Dilution buffer	Tween 20	0.05%
	BSA	0.1%
	Add 1x PBS	
Elution buffer, pH 2.7	Glycin-HCl	0.1 mol/L
Gel buffer 3.5x, pH 6.5-6.8	Bis-Tris	1.25 M
Glycin stripping buffer	Glycin	25 mM
pH 2.0	SDS	1% m/v
Laemmli buffer 5x	Tris-HCl, pH 7.5	250 mM
	DTT	500 mM
	Glycerol	30% v/v
	SDS	5% m/v
	Bromphenol blue	0.25% m/v
MOPS running buffer 1x, pH 7.7	MOPS	50 mM
	Tris	50 mM
	EDTA, pH 8.0	1 mM
	SDS	0.1% m/v
Neutralization buffer, pH 9.0	Tris	1 M
PBS (Ca^{2+}-/Mg^{2+}-free), pH 7.3	NaCl	137 mM
	KCl	2.7 mM
	Na_2HPO_4	9 mM
	KH_2PO_4	2.3 mM

Buffer	Reagent	Final Conc.
TBE buffer 1x,	Tris	89 mM
pH 8.0	Boric acid	89 mM
	EDTA	2 mM
TBS-T buffer 1x,	Tris	50 mM
pH 7.6-8.0	NaCl	150 mM
	Tween 20	0.1% v/v
TE buffer 10x	Tris-HCl, pH 7.5	0.1 M
	EDTA	0.01 M
TST lysis buffer	Tris-HCl, pH 8.0	100 mM
	SDS	0.2% m/v
	TritonX-100	1% v/v
TST lysis buffer	Roche Complete	0.1% v/v
	β-Glycerolphosphate	10 nM
	NaF	10 nM
	Na_3VO_4	1 nM
	Sodium pyrophosphate	10 nM
Wash buffer (ELISA)	Tween 20	0.05%
	Add 1x PBS	

3.1.7 Media

Media	Reagent	Final Conc.
LB medium	Bacto tryptone	1% m/v
	Bacto yeast extract	0.5% m/v
	NaCl	1% m/v
	sterilized by autoclaving	
LB agar plate	Bacto tryptone	1% m/v
	Bacto yeast extract	0.5% m/v
	NaCl	1% m/v
	Bacto agar	1.5% m/v
	sterilized by autoclaving	
HMEC-1 complete medium	L-glutamine	10 mM
	hEGF	10 ng/mL
	Hydrocortisone	10 nM
	FCS	5%v/v
	Penicillin	100 U/mL
	Streptomycin	100 µg/mL

Media	Reagent	Final Conc.
HMEC-1 starvation Medium	L-glutamine	10 mM
	hEGF	10 ng/mL
	Hydrocortisone	10 nM
	FCS	0.5% v/v
	Penicillin	100 U/mL
	Streptomycin	100 µg/mL

3.1.8 Primers

All primers were synthesized by TIB Molbiol (Germany) and dissolved in water with a final concentration of 100 µM.

The sequence of primers used for amplifying *PAR-2* cDNA was 5'-TACCGAGCTCGGATCCATGCGGAGCCCCAGCGCG-3' (Forward), and 5'-GATATCTGCAGAATTCCTAATAGGAGGTCTTAACAG-3' (Reverse). The sequence of the primer used for DNA sequencing was 5'-CGCAAATGGGCGGTAGGCGTG-3'. The sequence of the primers used for RT-qPCR are listed below in Table 1. All the primers were diluted at a concentration of 10 µM with ddH_2O before use.

Primer Name	5'→3'
B2M forward	GTGCTCGCGCTACTCTCTCT
B2M reverse	CGGCAGGCATACTCATCTTT
GAPDH forward	CCATCTTCCAGGAGCGAGAT
GAPDH reverse	GATGACCTTGCCCACAGCCT
PAR-2 forward	TGCTAGCAGCCTCTCTCTCC
PAR-2 reverse	CCAGTGAGGACAGATGCAGA
VEGFA forward	CCTTGCTGCTCTACCTCCAC
VEGFA reverse	CACACAGGATGGCTTGAAGA

Table 1. Primers for qRT-PCR

3.2 Methods

3.2.1 RNA extraction, cDNA production and qPCR

3.2.1.1 RNA extraction and cDNA production

Total RNA was extracted from cultured endothelial cells using Qiazol according to the manufacturer's protocol. RNA pellets were dissolved in diethyl pyrocarbonate (DEPC) water and

the concentration was measured by NanoDrop® Spectrophotometer. Absence of genomic DNA contamination in isolated RNA samples was confirmed by agarose gel electrophoresis.

1µg of total RNA was reverse-transcribed to cDNA by M-MuLV Reverse Transcriptase using Oligo dT primer. Reverse transcription components are shown in Table 2, and reverse transcription reaction conditions in Table 3.

Content	Final concentration
10X M-MuLV Reverse transcriptase Buffer	1X
dNTP mix (10 mM)	1.6 mM
RNase inhibitor (20 U/µL)	0.4 U/µL
M-MuLV Reverse transcriptase (200,000 U/mL)	1 U/µL
Oligo(dT)16 Primer (50 µM)	1 µM
RNA	0.02 µg/µL
ddH_2O	--
Total	--

Table 2. cDNA synthesis system

Temperature (℃.)	Time
25	10 min
40	1 hr
90	5 min

Table 3. Reverse transcription reaction conditions

3.2.1.2 qPCR

Quantitative PCR was performed to quantify the level of gene expression of a gene of interest with the Applied Biosystems® 7500 qRT-PCR System under the cycling conditions listed in Table 4. Quantitative PCR components are listed below in Table 5. To show the expression of *B2M* and *PAR-2* in HMEC-1 cells, qPCR products were collected and checked on TBE agarose gel.

Temperature (℃.)	Time
90	10 min
40	1 hr
90	5 min
4	--

Table 4. qPCR cycling condition

Content	Volume (1X)	Final concentration
SYBR Green	4 µL	1x
Forward Primer (10 µM)	0.5 µL	0,4 µM
Reverse Primer (10 µM)	0.5 µL	0,4 µM
ddH_2O	7 µL	--
cDNA	1 µL	--
Total	13 µL	--

Table 5. qPCR components

3.2.1.3 Agarose gel electrophoresis

1% TBE agarose gel was used for gel electrophoresis. Solidified agarose gel was placed into the gel box (electrophoresis unit) in TBE buffer. Samples were mixed with 6X DNA loading buffer and 1/50 Midori green direct DNA dye. Samples and DNA ladders were loaded into the wells and electrophoresed at 100 V for one hour before visualizing the bands under a UV-transilluminator.

3.2.2 Generation of PAR-2 expression constructs

3.2.2.1 PAR-2 amplification

PAR-2 was amplified using the CloneAmp HiFi PCR Premix using HMEC-1 cDNA as the template. PCR components are listed below in Table 6, and the cycling conditions are listed below in Table 7. Agarose gel electrophoresis was performed to confirm that a single DNA fragment with the expected size had been obtained.

Reagent	Volume/Quantity	Final Conc.
CloneAmp HiFi PCR Premix	12.5 µL	1X
10 µMForward Primer	5 pmol	0.2 µmol/L
10 µMReverse Primer	5 pmol	0.2 µmol/L
cDNA	2 µL	
Sterilized distilled water	up to 25 µL	

Table 6. PCR master mix

Temperature (°C)	Time (sec.)	Amplification cycles
98	60	--
98	10	35
60	10	35
72	15	35
72	60	--

Table 7. PCR cycling conditions

3.2.2.2 Vector linearization and purification

1µg of the pcDNA3.1 plasmid was linearized using 20 units of *BamH*I-HF and 20 units of *EcoR*I-HF restriction enzymes in CutSmart buffer provided by the manufacturer. Samples were incubated at 37°C for six hours and digestion was verified on a TBE agarose gel.

Linearized plasmid was purified using a PeqGOLD MicroSpin Cycle-pure kit according to the manufacturer's instructions. The concentration of purified vector was measured using a NanoDrop® Spectrophotometer.

3.2.2.3 PAR-2 cDNA insertion

An In-Fusion HD Cloning kit was used to insert *PAR-2* into the pcDNA3.1 linearized vector according to manufacturer's instructions. In brief, previously generated *PAR-2* cDNA generated previously was treated with the Cloning Enhancer according to the manufacturer's instructions. In-Fusion cloning reaction was set up as listed below in Table 8.

Component	Volume/quantity
5X In-Fusion HD Enzyme Premix	2 µL
Linearized Vector	100 ng
Enhancer-treated *PAR-2* cDNA	2 µL
ddH_2O	up to 10 µL

Table 8. In-Fusion cloning reaction

3.2.2.4 Bacterial transformation

Stellar™ competent cells were used as the host cells for generating multiple copies of plasmid DNA. Heat-shock transformation was used to introduce the foreign plasmid into the host cells. Transformation was performed according to the manufacturer's instructions. Transformed bacteria were plated onto a 10cm LB agar plate containing 100 µg/mL ampicillin for selection, and allowed to grow overnight in a 37°C incubator before picking bacteria colonies.

3.2.2.5 Recombinant plasmid isolation, verification and expansion

Colonies growing on the agar plate were picked and pre-cultivated into LB liquid medium containing ampicillin (100 µg/mL) overnight. 2 mL of every pre-culture were used for plasmid preparation. Plasmid preparation was carried out using the GeneJET Plasmid Miniprep Kit according to manufacturer´s instructions. The concentration of the isolated plasmids was measured

by NanoDrop® Spectrophotometer.

To assert *PAR-2* cDNA presence, isolated plasmids were digested with *Hin*dIII-HF and *Xho*I restriction enzymes at 37°C for three hours, and then checked by TBE agarose gel electrophoresis. Plasmids showing two bands corresponding to the size of the vector and the *PAR-2* cDNA were considered to be positive. The positive plasmids were sent to LGC Genomics GmbH for sequencing. The resulting sequences were analyzed using the NCBI standard nucleotide BLAST tool.

In order to obtain a large amount of plasmid, plasmid preparation was performed using the NucleoBond® Xtra Midi kit, following the protocol provided by the manufacturer. The plasmids were stored at -20°C prior to use.

3.2.3 PAR-2 IgG level measurement and IgG isolation

Measurement of the levels of autoantibodies against PAR-2 in serum from kidney transplant patients and healthy controls was performed by CellTrend GmbH, using a solid-phase based ELISA (ethical approval for serum samples: EA2/068/07). The CellTrend PAR-2 antibody ELISA is an antibody screening test. Human PAR-2 is pre-coated onto a microtiter plate, serving as antigen. During the first incubation the anti-PAR-2 antibodies of the samples are immobilised on the plate. The auto-antibodies are detected with a POD labeled anti-human IgG antibody. In the following enzymatic substrate reaction, the intensity of the colour correlates with the concentration and/ or avidity of anti-PAR-2 antibody.

Immunoglobulins (IgG) were purified by affinity chromatography using HiTrap Protein G columns. The serum was centrifuged at 5,000rpm for 15min, and filtered with 0.45µm PVDF syringe filters to remove the remaining cell debris, before diluting with the same volume of binding buffer. HiTrap Protein G column was equilibrated with binding buffer before loading samples into the column. To increase the recovery rate, flow through was collected and loaded again. After washing the column with binding buffer, captured IgG were eluted with elution buffer, and the collected IgG was neutralized immediately using neutralization buffer.

Purified IgG was dialyzed against DMEM low glucose medium overnight under constant stirring at 4°C. After dialysis, the concentration of IgG was determined by Labor Berlin.

3.2.4 Cell experiments

3.2.4.1 HMEC-1 cell culture

HMEC-1 were grown on gelatin pre-coated flask or plates in HMEC-1 complete medium in a humidified incubator at 37°C with 5% CO_2 and were used between passage 21 and 30. Cells at 90% confluence were trypsinized with Trypsin-EDTA solution. After centrifugation and resuspension in complete medium, the harvested cells were counted with a Neubauer cell chamber in the presence of Trypan blue to assess their viability. 50,000 cells or 200,000 cells in HMEC-1 complete medium were seeded per well, in 24 well plates or 6 well plates, respectively. 1,000,000 cells in HMEC-1 complete medium were seeded in a 75 cm^2 flask. 500,000 cells HMEC-1 cells were seeded in complete medium into 6 cm^2 dishes.

3.2.4.2 Cell stimulation

Cells at 70 to 80% confluence were serum-starved overnight prior to stimulation. For the VEGF ELISA experiment, cells were stimulated with 100 nM trypsin or 1 mg/mL IgG for 24 hours, and then medium was collected. For mRNA expression experiments, cells were stimulated for the indicated time period using appropriate stimuli. For receptor blocking experiments, cells were pre-incubated with specific receptor blocker(s) for one hour before addition of stimuli.

3.2.4.3 Luciferase reporter assay

Cells were allowed to grow for 3 days to reach a confluence of 80-90% before transfection. Cells were transiently transfected with 100 ng serum response element (SRE), or 100 ng serum response factor (SRF), or 200 ng nuclear factor of activated T-cells (NFAT) reporter plasmid per well, in 24 well plates using Xfect transfection reagent according to manufacturer's instructions. To overexpress *PAR-2*, rising amounts of pcDNA-PAR-2 plasmid were co-transfected. Four hours after transfection, the medium was changed to HMEC-1 starvation medium, and cells were further cultured in the incubator. After 24 hours of transfection, cells were stimulated with isolated IgG, trypsin or DMEM low glucose as a control. After 6 hours stimulation, cells were washed twice thoroughly with PBS, and then lysed with 100µL of 1X PLB at room temperature for 15min under constant shaking. Luciferase activity in the cell lysates was detected using the Luciferase Assay

System from Promega according to manufacturer's instructions with a FLUOstar microplate reader.

3.2.4.4 Dual luciferase reporter assay

For dual reporter assay, 100 ng of *VEGF*2068 promoter-luciferase plasmid and 2 ng of Renilla control vector were transfected per well in 24 well plates using Xfect transfection reagent. To overexpress *PAR-2*, 100 ng of pcDNA-PAR-2 plasmid were co-transfected. Four hours after transfection, the medium was changed to HMEC-1 starvation medium, and cells were further cultured in the incubator. 24 hours after transfection, cells were stimulated for 6 hours. Then, cells were washed twice thoroughly with PBS, and lysed with 100 µL of 1X PLB. Luciferase activity in the cell lysates was detected using the Dual-Luciferase® Reporter (DLR™) Assay System from Promega according to manufacturer's instructions with a FLUOstar microplate reader.

3.2.4.5 Matrigel angiogenesis assay

Frozen basement membrane extract gels were placed in a refrigerator at 4°C and allowed to thaw overnight. A pre-cooled 96-well cell culture plate was coated with 50 µL thawed matrigel each well using chilled 200 µL pipette tips. The 96-well plate was put into the cell culture incubator and incubated at 37°C for 30 min.

80%-90% confluent HMEC-1 cells from the 75-cm^2 flask were harvested and resuspended in HMEC-1 starvation medium. Cell number was determined using the tryptan blue exclusion method. Cells were furthered diluted with HMEC-1 starvation medium to get a concentration of 2.0×10^5 cells per mL.

IgG was diluted with DMEM low glucose medium to reach a concentration of 2.0 mg/mL. 100 µL of IgG solution and 100 µL of cell suspension was then mixed gently by pipetting up and down a few times. Cells were then added on top of gelled basement membrane extract to begin the assay, and the 96-well plate was placed back into the incubator to allow the formation of capillary-like tubes.

After 16 h incubation, tubular formation of HMEC-1 was photographed using a camera, and was analyzed using the "Angiogenesis Analyzer" tool from Image J software. Total master segments length, which means the sum of the length of the detected master segments in the analyzed area,

was chosen as the parameter to represent the formation of the vascular structure.

3.2.5 VEGF ELISA

The concentration of VEGF in the supernatants was measured with the Human VEGF 165 Standard TMB ELISA Development Kit according to manufacturer´s instructions. The TMB and stop solution used were from the Antibody Pair Buffer Kit and prepared as recommended. Capture antibody was coated onto F16 Maxisorp loose Nunc-Immuno Modules overnight at room temperature. Samples were measured in duplicate, and 100 µL of supernatant was used for each measurement. After stopping the enzyme activity with sulfuric acid, absorbance at 450 nm (reference absorbance: 650 nm) was measured using a Thermo Multiskan Ascent 96 plate reader. The standard curve was plotted, linear regression was applied, and then the concentration of samples was calculated.

3.2.6 Western blot

After washing with PBS twice, cells were collected by scraping and lysed with TST lysis buffer for 30 min on ice. Supernatants containing total proteins were collected by centrifugation. Protein concentration determination was performed using Bio-Rad Protein Assay according to the manufacturer's guidelines. 30 µg protein/lane were subjected to Bicine/Tris gels and run with MOPS buffer under reducing conditions in a mini PROTEAN® Tetra cell. Proteins were transferred to a PVDF membrane in a Trans-Blot® cell with BICIN transfer buffer. After transferring, the membranes were blocked. The membranes were incubated with the respective primary antibody dissolved in 3% BSA TBS-T buffer overnight at 4°C. After washing, membranes were incubated with a secondary antibody. After additional washing steps, the bands were visualized with an enhanced chemiluminescence substrate according to the manufacturer's instructions on Syngene's automated gel documentation systems. In order to reuse the membranes for subsequent protein probing, membranes were rinsed and then incubated with stripping buffer. After further washing steps and a blocking step, the membranes could be re-used.

3.2.7 Statistical analysis

Data are expressed as mean ± SEM, n stands for the number of independent experiments.

Comparisons were performed by t-test. Differences were considered significant when the p value was smaller than 0.05. GraphPad Prism software version 7.01 was used for graphs and statistical analyses.

4 Results

4.1 Level of PAR-2-IgG in healthy individuals and renal transplant patients

The presence of autoantibodies directed against PAR-2 in healthy individuals and kidney transplantation patients (KTx patients) was detected by ELISA. The mean level of PAR-2-IgG was 17.68 units, and median value was 15.24 units/mL among 197 serum samples from healthy controls. The titer of PAR-2-IgG in KTx patients (n=6) was lower, with a mean value of 4.5 U/mL (Figure 5).

For PAR-2 autoantibodies, no cut-off values are available so far from the literature like for PAR-1 or other GPCR autoantibodies. In this study, the variation of PAR-2 levels was much less from KTx patients compared to healthy controls, and the mean values separated clearly. To keep experiments as representative as much as possible, PAR-2^- and PAR-2^+-IgG were used which were close to the median.

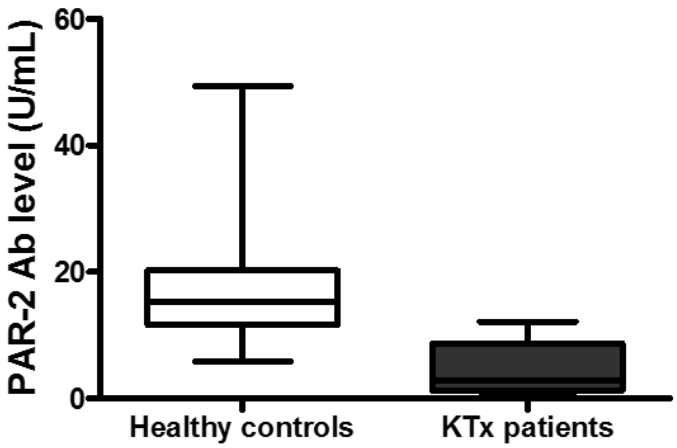

Figure 5. Measurement of the titers of PAR-2-IgG in healthy individuals and KTx patients. The 197 serum samples from healthy individuals were provided by the Celltrend Company. Kidney transplantation patients were patients who received at least one kidney transplant before sample collection. PAR-2-IgG levels were detected using Celltrend PAR-2 auto-antibodies ELISA kit.

4.2 Generation of PAR-2 overexpression HMEC-1 cells

4.2.1 Expression of PAR-2 in HMEC-1 cells

Although the expression of PAR-2 in endothelium in various organs and primary endothelial cells has been assessed, the presence of PAR-2 in HMEC-1 has not been reported yet. Using qRT-PCR, the expression of *PAR-2* mRNA in HMEC-1 was detected (Figure 6). Western blot showed the presence of PAR-2 (Figure 7).

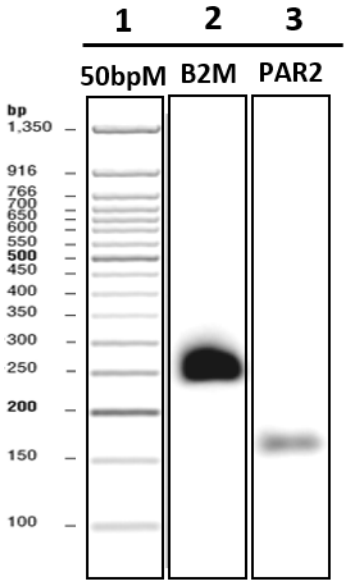

Figure 6. RT-PCR analysis of *PAR-2* expression in HMEC-1. Lane 1, 50bp Generuler DNA ladder; lane 2, *B2M* fragment (272 bp); lane 3, *PAR-2* fragment (184 bp).

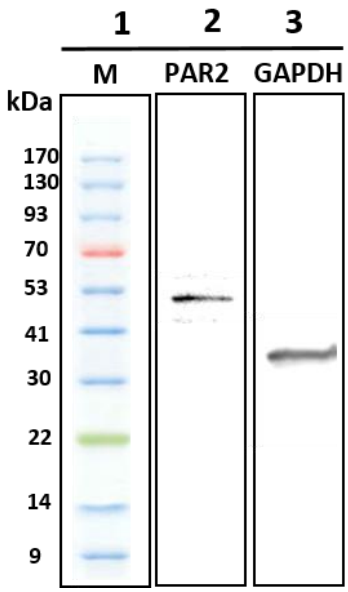

Figure 7. Western blot analysis of PAR-2 expression in HMEC-1. Lane 1, PageRuler prestained protein marker; lane 2, PAR-2 (50kDa); lane 3, GAPDH (36 kDa) used as reference protein.

4.2.2 Generation of pcDNA-*PAR-2* construct

The pcDNA3.1 plasmid containing a CMV promoter (Figure 8) was used to overexpress the human *PAR-2* in HMEC-1. The ampicillin resistance gene within the plasmid allows antibiotic selection in *E. coli*.

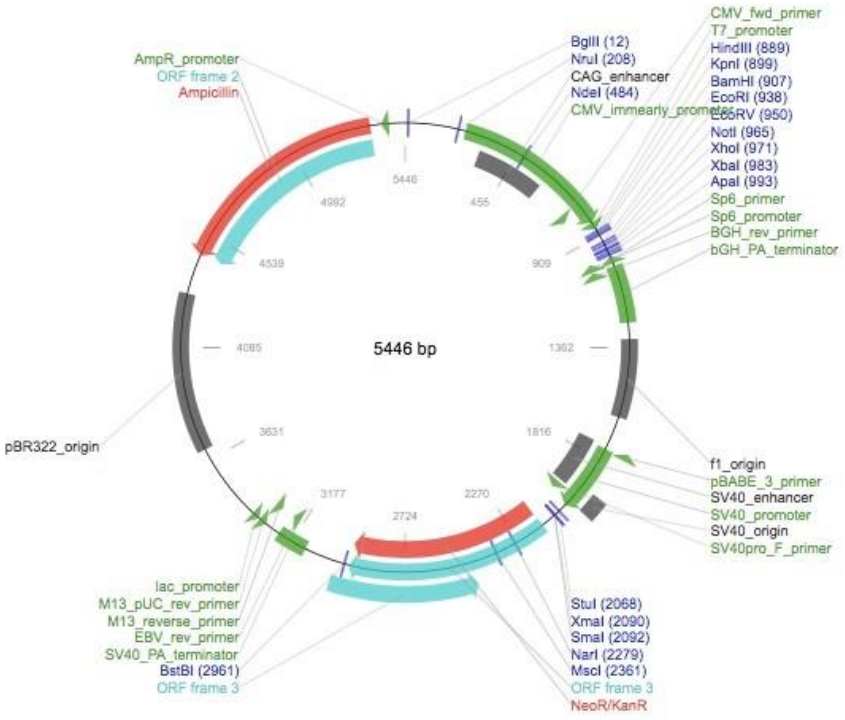

Figure 8. Map of the pcDNA3.1 plasmid (5446 base pairs). (50)

*BamH*I and *EcoR*I restriction enzymes were used for plasmid linearization. As shown in Figure 9, full-length *PAR-2* cDNA was successfully amplified from HMEC-1 cDNA using PCR primers designed with 5' 15-bp extensions homologous to the ends of the linearized vector, facilitating the ligation between insert and linearized vector. *PAR-2* cDNA was ligated in the linearized vector, and plasmid DNA product was transformed into competent bacteria.

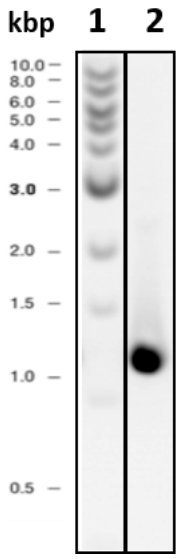

Figure 9. Agarose gel electrophoresis of full length *PAR-2* cDNA from HMEC-1 cDNA**.** Lane 1, 1kb DNA ladder; lane 2, *PAR-2* PCR product.

To verify the insertion of *PAR-2* into the pcDNA3.1 vector, plasmids were digested with *Hin*dIII-HF and *Xho*I restriction enzymes. As shown in Figure 10, a recombinant plasmid, representative of the *PAR-2* containing plasmids, (lane 4) migrated more slowly than the wild-type plasmid (lane 2), indicating a bigger size. After restriction, the wild-type pcDNA3.1 plasmid (lane 3) showed a single band of the expected size (5446 bp), while the plasmid with *PAR-2* cDNA (lane 5) showed two bands, with a smaller band between 1000 bp and 1500 bp corresponding to the *PAR-2* insert (1191 bp).

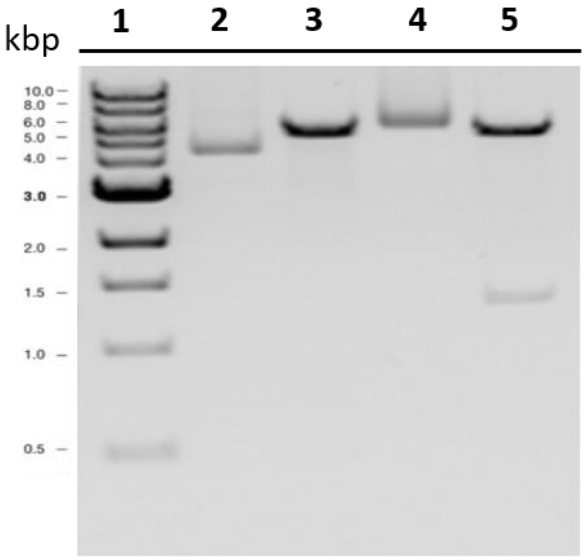

Figure 10. Agarose gel electrophoresis of digested or undigested plasmid. Lane 1, 1kb DNA ladder; lane 2, undigested wild-type pcDNA plasmid; lane 3, digested wild-type pcDNA plasmid; lane 4, undigested pcDNA-*PAR-2* plasmid; lane 5, digested pcDNA-*PAR-2* plasmid.

4.2.3 Confirmation of PAR-2 overexpression after transient transfection

To confirm *PAR-2* overexpression after pcDNA-*PAR-2* plasmid transient transfection in HMEC-1, the *PAR-2* mRNA level of transiently transfected cells was analyzed by qRT-PCR. *PAR-2* mRNA was expressed around 75-fold more in transiently transfected cells in comparison to cells transfected with wild-type pcDNA 3.1 alone. (Figure 11).

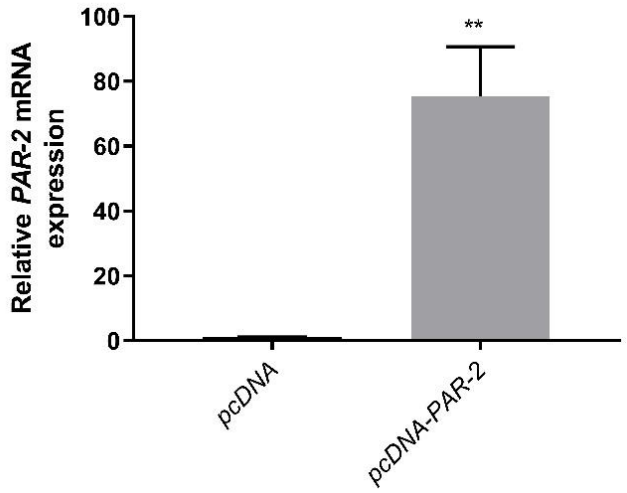

Figure 11. Effect of pcDNA-*PAR-2* plasmid transfection on *PAR-2* mRNA level. Cell were lyzed and total RNA was extracted 24 hours after plasmid transfection. qRT-PCR was performed to measure the level of *PAR-2* mRNA. Data are presented as mean ± SEM. ** $p < 0.01$ vs. pcDNA control, n=3.

4.3 Activation of G-protein signaling and MAPKs signaling by stimulated PAR-2

4.3.1 Increased G-protein activity upon PAR-2 activation

Upon activation of GPCRs, activation of G protein α subunit initiates a cascade of downstream second messenger pathways and eventually induces gene transcription by various response elements.(51) Thus, activation of response elements can reflect the activation of a certain G protein α subunit pathway. Luciferase reporter assay using reporter vectors with different response elements built in upstream of luciferase gene can be applied to monitor GPCR signaling events.(51) (Figure 12).

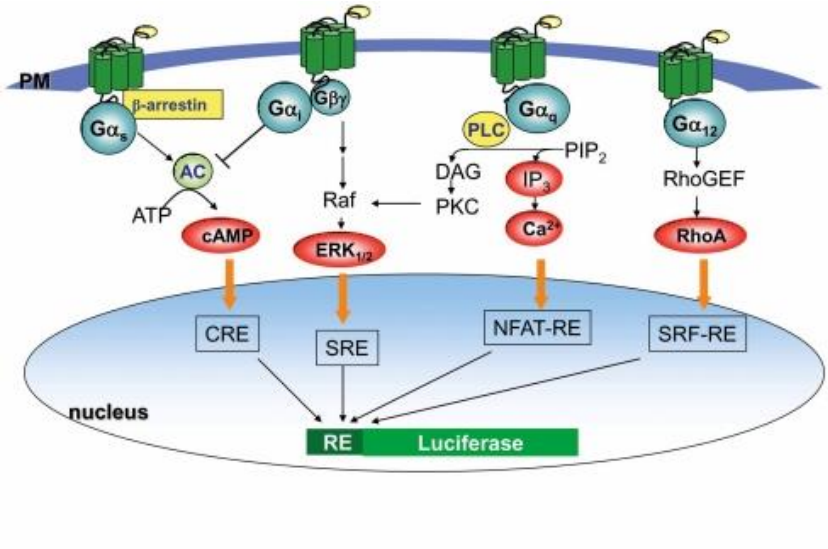

Figure 12. Schematic diagram showing major GPCR signaling pathways, and the activation of various response elements. (51)

In order to show that PAR-2 in HMEC-1 was functional, a luciferase reporter assay was performed. Activation of ERK1/2 signaling pathway, $G_{\alpha 12/13}$, and G_q protein pathways by PAR-2 has been reported. To assess the activation of these pathways, HMEC-1 were transiently transfected with SRE, SRF or NFAT luciferase reporter plasmids, which can be used to monitor ERK1/2, $G_{\alpha 12/13}$ or G_q signaling pathway, respectively.

4.3.1.1 Increased G-protein activity by trypsin treatment

First, we investigated the activation of SRE, SRF and NFAT reporter plasmids by trypsin. Trypsin increased both SRE and SRF reporter plasmid activity in a dose dependent manner, indicating ERK1/2 and $G_{\alpha 12/13}$ activation (Figure 13). Activation of NFAT luciferase activity (G_{q11} activation) could not be detected at the tested concentration (data not shown). However, when the pcDNA-*PAR-2* plasmid was co-transfected, 100nM trypsin stimulation increased the NFAT luciferase activity (G_{q11} signaling activation) by 72%. (Figure 14)

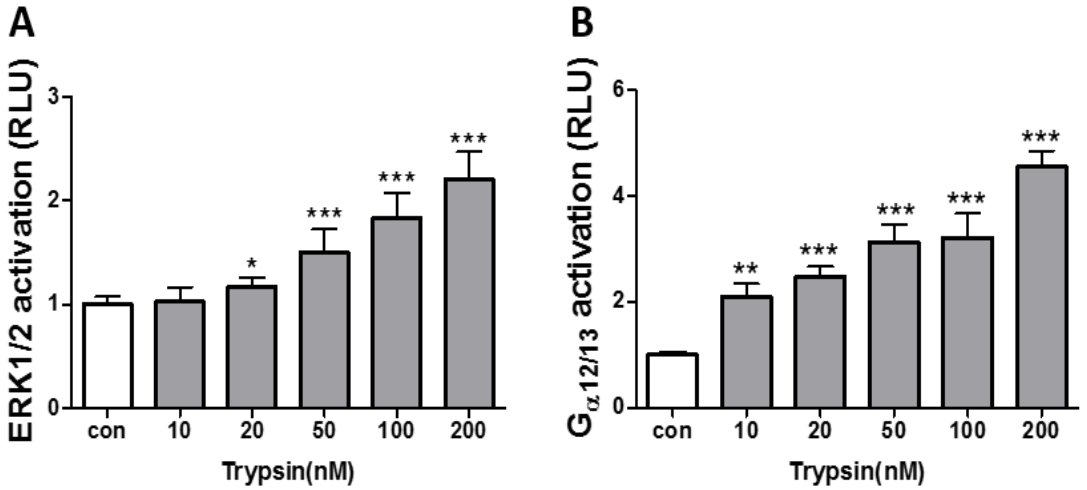

Figure 13. Activation of ERK1/2 (A) and $G_{\alpha 12/13}$ (B) by increasing doses of trypsin. ERK1/2 activation (RLU) is depicted as the activity of SRE luciferase in cells treated with trypsin relative to SRE luciferase activity without stimulation. $G_{\alpha 12/13}$ activation (RLU) is depicted as the activity of SRF luciferase in cells treated with trypsin relative to SRF luciferase activity without stimulation. Data are presented as mean ± SEM. * $p < 0.05$, ** $p < 0.01$, *** $p < 0.001$ vs. con, n=6 in (A) and n=3 in (B).

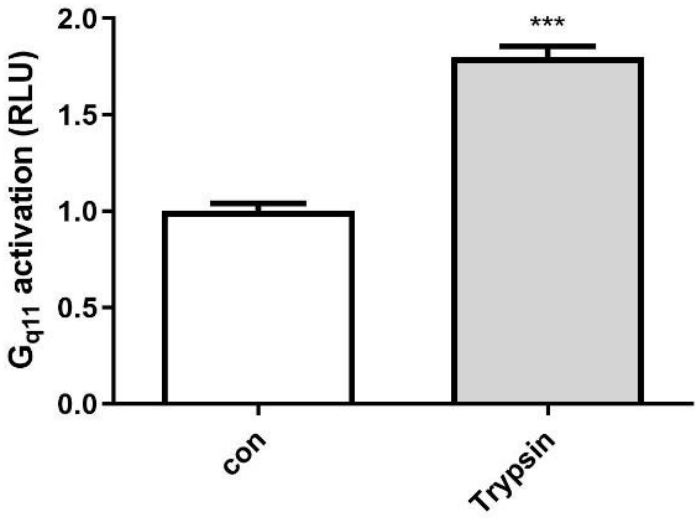

Figure 14. Effect of trypsin on G_{q11} signaling activation. G_{q11} activation (RLU) is depicted as the activity of NFAT luciferase in cells treated with trypsin relative to NFAT luciferase activity without stimulation. Data are presented as mean ± SEM. * $p < 0.05$, ** $p < 0.01$, *** $p < 0.001$ vs. con, n=6.

pcDNA-*PAR-2* transfection increased the mRNA level of *PAR-2*. We analyzed the consequence of PAR-2 overexpression on basal G-protein activity and the signaling activity in response to trypsin.

PAR-2 overexpression itself slightly elevated the basal SRE activity. The fold change of SRE luciferase activity on trypsin stimulation increased from 1.7-fold to 7.6-fold when 50ng of pcDNA-*PAR-2* plasmid were co-transfected. The fold change was 9.3 when 150ng of pcDNA-*PAR-2*

plasmid were co-transfected with SRE plasmid. Thus, PAR-2 overexpression may facilitate the recruitment of G protein, consequently leading to a more potent G-protein signaling pathway activation upon ligand binding to PAR-2. (Figure 15)

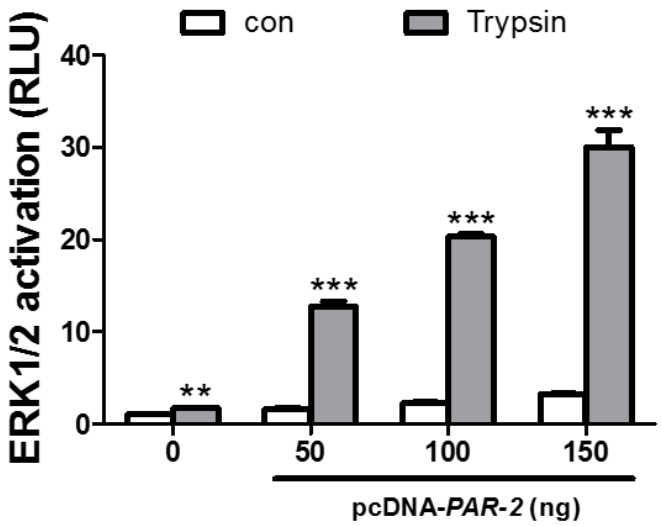

Figure 15. Effect of PAR-2 overexpression on ERK1/2 signal activation. Cells were transfected with different amounts of wild-type pcDNA and pcDNA-*PAR-2* plasmid. ERK1/2 activation (RLU) is depicted as relative to SRE luciferase activity from cells transfected with 150ng pcDNA plasmid in the absence of trypsin stimulation. Data are presented as mean ± SEM. * $p < 0.05$, ** $p < 0.01$, *** $p < 0.001$ vs. con, n=3.

PAR-2 overexpression had no effect on the basal SRF luciferase activity, indicating that PAR-2 overexpression itself did not lead to constitutive $G_{\alpha 12/13}$ activation. However, the relative fold change increased from 2.1-fold to 14-fold when 50ng of pcDNA-*PAR-2* plasmid was co-transfected. The fold change was 47.0 when 150ng of pcDNA-*PAR-2* plasmid were co-transfected along with SRF luciferase plasmid. Thus, PAR-2 overexpression may facilitate the recruitment of $G_{\alpha 12/13}$ protein, therefore more potently activating the G-protein signaling pathway upon receptor activation. (Figure 16)

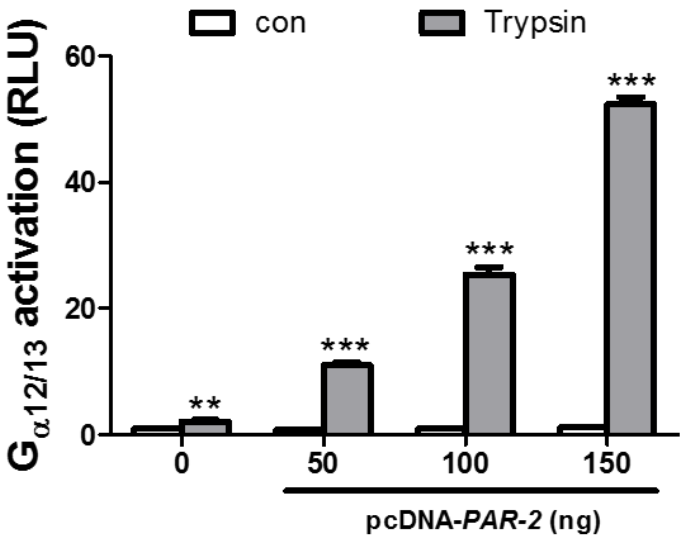

Figure 16. Effect of PAR-2 overexpression on $G_{\alpha 12/13}$ activation signal activation. Cells were transfected with different amounts of pcDNA and pcDNA-PAR-2 plasmid. $G_{\alpha 12/13}$ activation (RLU) is depicted as relative to SRF luciferase activity from cells transfected with 150ng pcDNA plasmid in the absence of trypsin stimulation. Data are presented as mean ± SEM. * $p < 0.05$, ** $p < 0.01$, *** $p < 0.001$ vs. con, n=3.

4.3.1.2 Increased G-protein activity by PAR-2 AP treatment

To avoid the possibility that trypsin may lead to activation of other cell membrane receptors, we chose PAR-2 AP as agonist and investigated its effect on G protein activation. PAR-2 AP activated both the ERK1/2 and $G_{\alpha 12/13}$ signaling pathways, and this regulation was dose-dependent (Figures 17 and 18). It led to an ERK1/2 activity increase by 1.3-fold without PAR-2 overexpression (Figure 17A).100µM of PAR-2 AP increased ERK1/2 activity by 7.2-fold when PAR-2 was overexpressed (Figure 17B). 50µM of PAR-2 AP increased $G_{\alpha 12/13}$ signaling activity by 8-fold when cells were transfected with 100 ng of pcDNA-*PAR-2* plasmid (Figure 18B). It also led to $G_{\alpha 12/13}$ activation by 1.3-fold when PAR-2 was not overexpressed (Figure 18A).

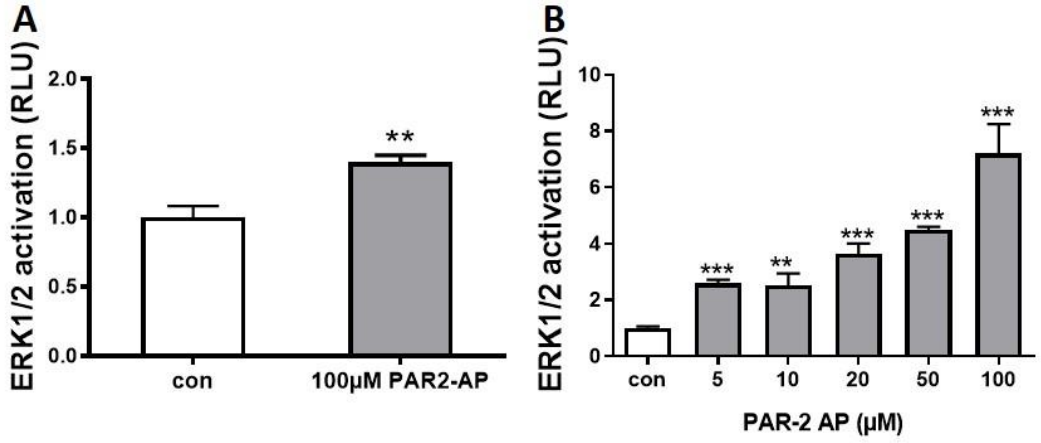

Figure 17. Effect of PAR-2 AP on ERK1/2 signal activity. A: effect of 100 μM PAR-2 AP on ERK1/2 activation (RLU). PAR-2 was not overexpressed in these cells. B: dose dependent effect of PAR-2 AP on ERK1/2 activation (RLU). PAR-2 was overexpressed in these cells. ERK1/2 activation (RLU) is depicted as relative to SRE luciferase activity of cells in the absence of PAR-2 AP stimulation. Data are presented as mean ± SEM. * $p < 0.05$, ** $p < 0.01$, *** $p < 0.001$, n=3 in (A) and (B).

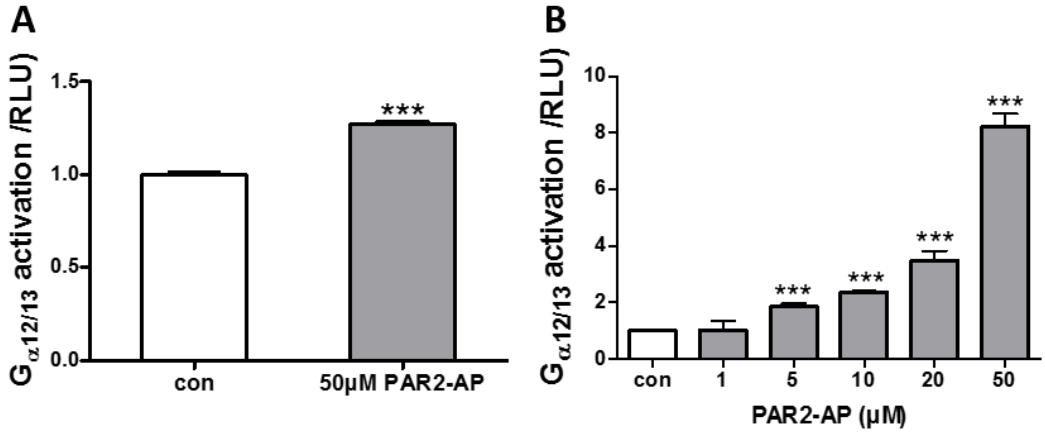

Figure 18. Effect of PAR-2 AP on $G_{\alpha 12/13}$ signal activity. A: effect of 50 μM PAR-2 AP on $G_{\alpha 12/13}$ activation (RLU). PAR-2 was not overexpressed in these cells. B: dose dependent effect of PAR-2 AP on $G_{\alpha 12/13}$ activation (RLU). PAR-2 was overexpressed in these cells. $G_{\alpha 12/13}$ activation (RLU) is depicted as relative to SRF luciferase activity of cells in the absence of PAR-2 AP stimulation. Data are presented as mean ± SEM. * $p < 0.05$, ** $p < 0.01$, *** $p < 0.001$, n=3 in (A) and (B).

4.3.2 Activation of MAKPs and Akt signaling pathways by stimulated PAR-2

PAR-2 is reported to activate MAPKs and Akt signaling pathways in various cell lines. As shown in Figure 19, 100 nM of trypsin led to activation of the ERK1/2, p38 and Akt pathways. Phosphorylation of ERK1/2 was significantly increased at 5min, and decreased thereafter. Phosphorylation of p38 could be seen at 5 min, and remained at a high level after 1 hour.

Phosphorylation of Akt at Thr 308 and Ser 473 was evident at 5min, and dropped gradually until 15min to basal level. It increased again after 30min, and remained higher than the untreated group until one hour had elapsed

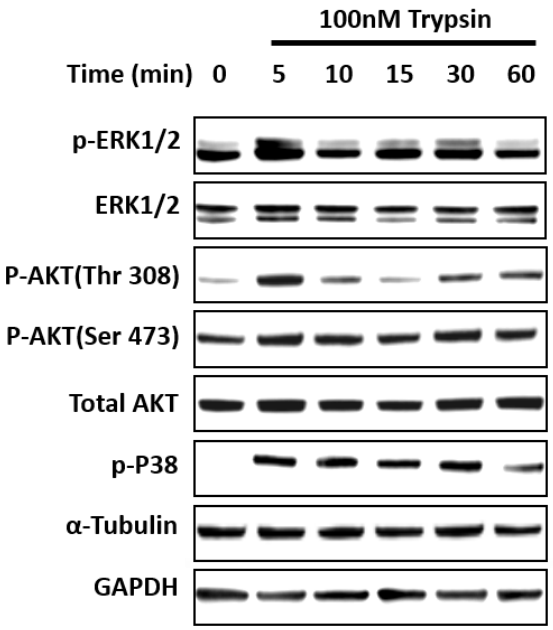

Figure 19. Effect of 100nM Trypsin treatment on MAPKs and Akt phosphorylation**.** Cells grown in serum-free medium were treated without 100nM trypsin for the indicated time point; untreated cells were used for time point 0 min. Lysates from treated or untreated cells were tested for ERK1/2, p38, or Akt phosphorylation.

The results from this section showed that PAR-2 activation by trypsin and PAR-2 AP triggered the activation of various G-protein signaling, including $G_{\alpha 12/13}$ and G_q proteins. The ERK1/2, p38 and Akt signaling pathways were all activated by trypsin treatment.

4.4 Regulation of VEGF expression at mRNA and protein levels by trypsin

To investigate the effect of PAR-2 activation on VEGF synthesis and release, the effect of trypsin on the VEGF protein level was first studied. The VEGF level in the supernatant from trypsin treated cells was 280 pg/mL, which was significantly higher than with untreated cells (210 pg/mL) (Figure 20).

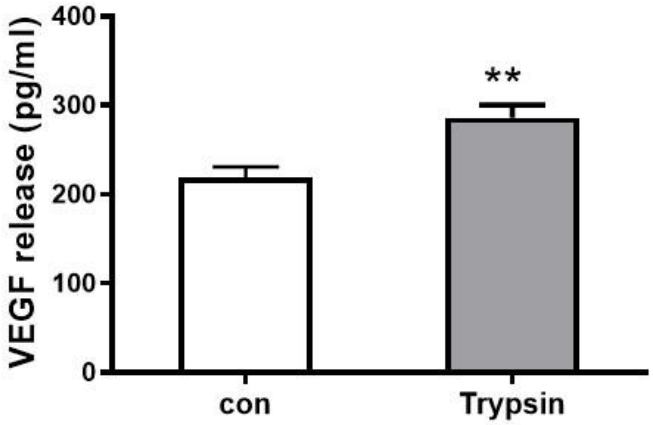

Figure 20. Effect of trypsin on VEGF release**.** Cells were starved overnight before stimulation with 100nM trypsin. Supernatants were collected 24 hours later and the VEGFA level was measured by ELISA. Data are presented as mean ± SEM. ** $p < 0.01$ vs. con, n=3.

qRT-PCR was performed to investigate whether trypsin treatment could elevate the *VEGF* mRNA level. 20nM trypsin was sufficient to increase the *VEGF* mRNA level after six hours. The maximum stimulatory effect was seen with 50nM, where the *VEGF* mRNA level increased to 1150% (Figure 21). The effect of trypsin on *VEGF* mRNA was blocked by ENMD 1068, a PAR-2 antagonist (Figure 22).

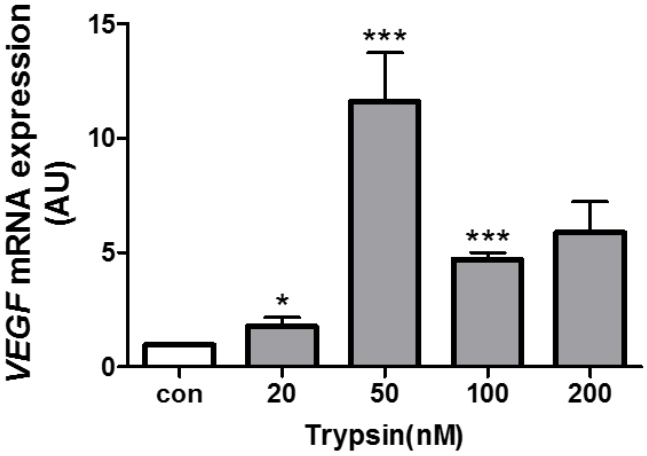

Figure 21. Effect of different doses of trypsin on the *VEGF* mRNA level**.** *VEGF* mRNA expression was calculated using *GAPDH* mRNA as reference; the relative *VEGF* mRNA level of untreated group was set as 1.0. Data are presented as mean ± SEM. * $p < 0.05$, ** $p < 0.01$, *** $p < 0.001$ vs. con, n=3.

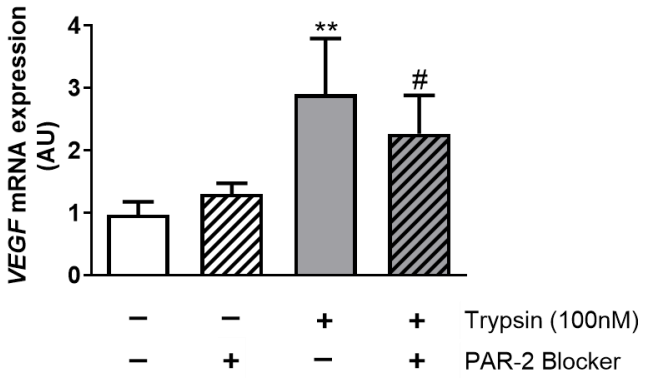

Figure 22. Effect of PAR-2 blocker on trypsin-induced *VEGF* mRNA level. Cells were stimulated with 100nM trypsin. PAR-2 blocker (50 μg/mL) was added 1 hour prior to trypsin stimulation. Total mRNA was extracted three hours after stimulation. Data are presented as mean ± SEM. ** $p < 0.01$ trypsin vs. con, # $p < 0.05$ trypsin plus PAR-2 blocker vs. trypsin, n=3.

Results from this section showed that trypsin increased the mRNA and protein level of VEGF, and this elevation was partially blocked by PAR-2 antagonist, ENMD 1068.

4.5 Functional characterization of PAR-2$^+$-IgG

4.5.1 Activation of GPCR signaling pathways by PAR-2$^+$-IgG

PAR-2-IgG levels differed between healthy individuals and KTx patients; whether these two IgG levels could activate the GPCR signaling pathway differently was unknown. As shown below in Figure 23, HC-IgG (PAR-2$^+$-IgG) strongly increased SRE, SRF and NFAT activity, while KTx-IgG (PAR-2$^-$-IgG) only activated SRF. The effect of PAR-2$^+$-IgG was also dose-dependent (Figure 24).

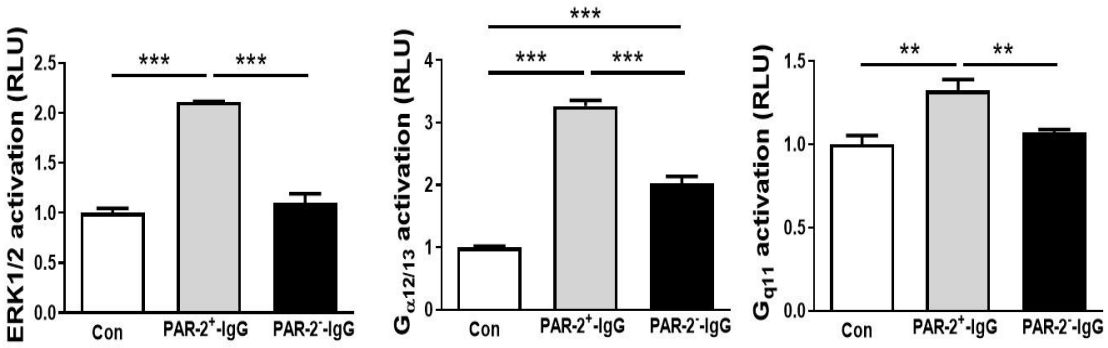

Figure 23. Effect of PAR-2$^+$-IgG and PAR-2$^-$-IgG on ERK1/2 (A), $G_{\alpha 12/13}$ (B) or G_{q11}(C) luciferase activity. IgG were used at a final concentration of 1mg/mL, control cells were treated with DMEM low glucose. Relative luciferase unit (RLU) is depicted as relative to luciferase activity from cells treated with DMEM low glucose. Data are presented as mean ± SEM. * $p < 0.05$, ** $p < 0.01$, *** $p < 0.001$vs con, n=4 in (A), (B) and (C).

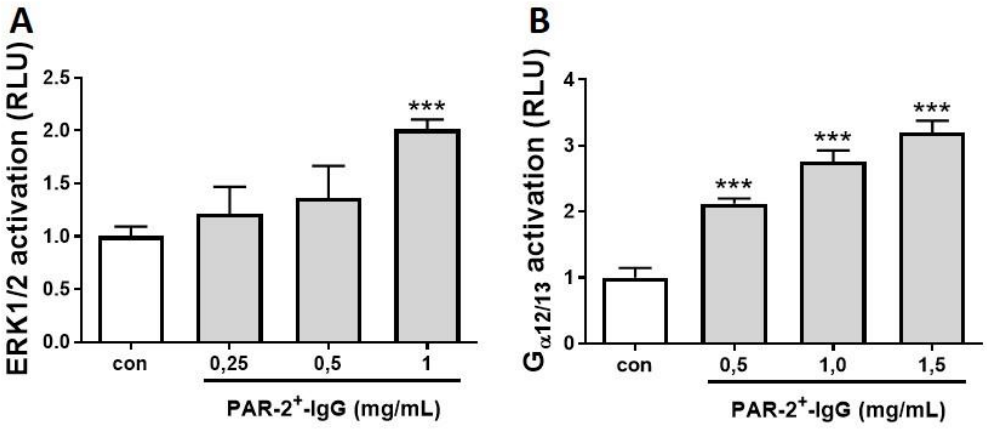

Figure 24. Effect of different doses of PAR-2$^+$-IgG on ERK1/2 and $G_{\alpha 12/13}$ signal activity. ERK1/2 activation (RLU) is depicted as relative to SRE luciferase activity from cells treated with DMEM low glucose. $G_{\alpha 12/13}$ activation is depicted as relative to SRF luciferase activity from cells treated with DMEM low glucose. Data are presented as mean ± SEM. * $p < 0.05$, ** $p < 0.01$, *** $p < 0.001$ vs con, n=3 in (A) and (B).

4.5.2 Activation of MAPKs and Akt signaling pathways by PAR-2$^+$-IgG

As the levels of PAR-2-IgG were more elevated in HC than in KTx patients, the effect of PAR-2$^+$-IgG on the ERK1/2, p38 and Akt signaling pathways was then investigated. As shown in Figure 25, PAR-2$^+$-IgG stimulation induced the phosphorylation of ERK1/2, Akt and p38 after 5 and 10 min.

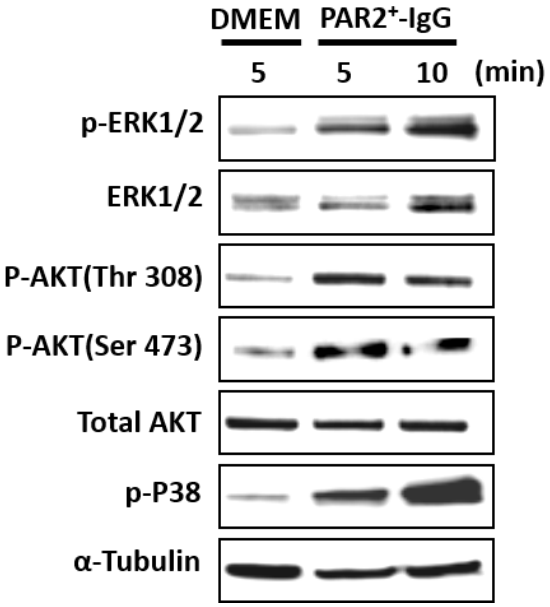

Figure 25. Effect of PAR-2$^+$-IgG on the ERK1/2, Akt and p38 signaling pathways. Cells grown in starvation medium were stimulated with DMEM low glucose medium or PAR-2$^+$-IgG (1mg/mL), and cells were lysed 5 min or 10 min after PAR-2$^+$-IgG or DMEM low glucose treatment. Lysates from treated or untreated cells were tested for ERK1/2, p38, or Akt phosphorylation.

4.6 Upregulation of *VEGF* mRNA and protein levels by PAR-2- IgG

4.6.1 Increase of VEGF protein level by PAR-2-IgG

The effect of IgG treatment on the VEGF protein level was analyzed. Incubation of the cells with 1 mg/mL PAR-2$^+$-IgG for 24 hours significantly increased the VEGF protein concentration in the medium, while PAR-2$^-$-IgG had no effect (Figure 26). Pre-incubation with PAR-2 blocker decreased the VEGF protein level. The effect of PAR-2$^+$-IgG on VEGF release was dose-dependent (Figure 27).

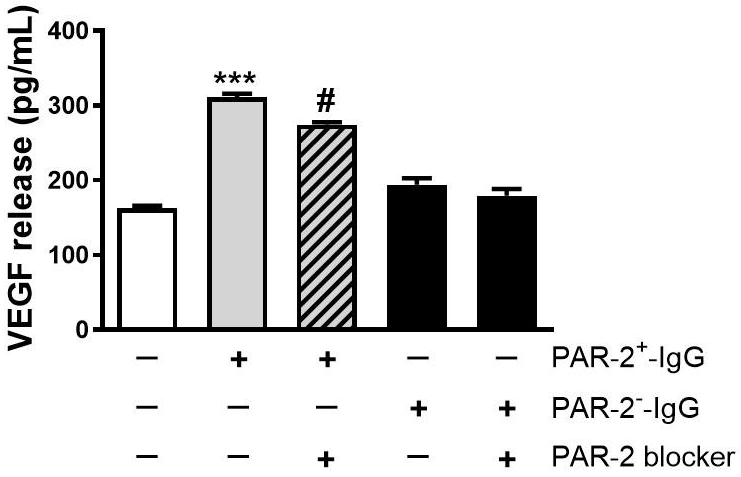

Figure 26. Effect of PAR-2$^+$-IgG and PAR-2$^-$-IgG on VEGF release. Cells were stimulated with 1mg/mL IgG or DMEM low glucose as control. 50µg/mL ENMD1068, the PAR-2 blocker, was added one hour prior to IgG stimulation. Supernatants were collected 24 hours later. Data are presented as mean ± SEM. *** $p < 0.005$ vs. con, # $p < 0.01$ PAR-2$^+$-IgG plus PAR-2 blocker vs PAR-2$^+$-IgG, n=3.

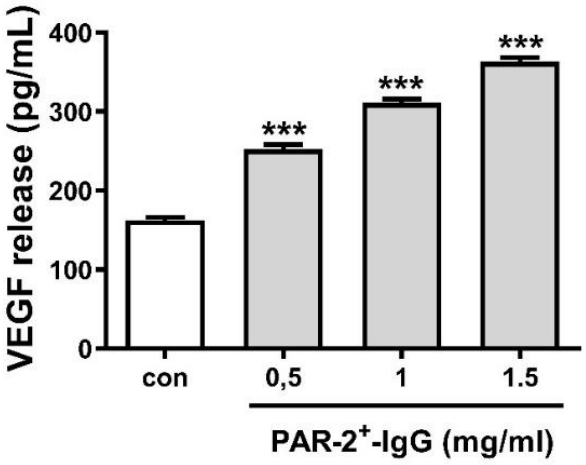

Figure 27. Effect of different doses of PAR-2$^+$-IgG on VEGF release. Supernatants were collected 24 hours after PAR-2$^+$-IgG stimulation and used for ELISA. Data are presented as mean ± SEM. *** $p < 0.005$ vs. con, n=3.

4.6.2 Increase of *VEGF* mRNA by PAR-2$^+$-IgG

Given that fact that PAR-2-IgG increased the VEGF protein level and that trypsin increased the *VEGF* mRNA level, PAR-2-IgG might upregulate the *VEGF* mRNA level. The effect of PAR-2$^+$-IgG on the *VEGF* mRNA level was measured. As shown in Figure 28, PAR-2$^+$-IgG stimulation led to a 17.6-fold increase in *VEGF* mRNA. Pre-incubation with the PAR-2 blocker significantly decreased the *VEGF* mRNA level compared to cells treated with IgG alone, indicating that PAR-2-IgG could increase *VEGF* mRNA in HMEC-1.

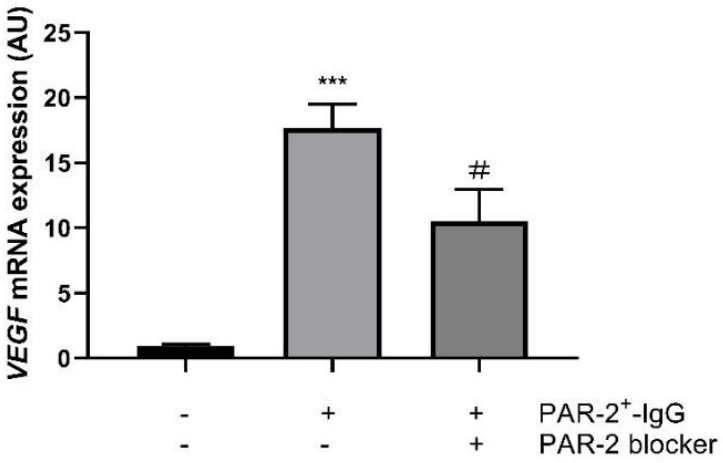

Figure 28. Effect of PAR-2$^+$-IgG treatment on the *VEGF* mRNA level. Cells were stimulated with 1mg/mL PAR-2$^+$-IgG. PAR-2 blocker was added one hour prior to stimulation. mRNA was isolated six hours post stimulation. Data were presented as mean ± SEM. *** $p < 0.001$ PAR-2$^+$-IgG group vs con, # $p < 0.05$ PAR-2$^+$-IgG plus PAR-2 blocker group vs PAR-2$^+$-IgG group, n=3

4.6.3 Upregulation of *VEGF* mRNA by PAR-2$^+$-IgG via p38 and ERK1/2 signaling pathways

PAR-2$^+$-IgG treatment activated both the p38 and ERK1/2 signaling pathways, thus these two signaling pathways might have critical effects on *VEGF* mRNA levels. As shown in Figure 29, both p38 and ERK1/2 inhibitors decreased PAR-2$^+$-IgG induced *VEGF* mRNA, indicating that both signaling pathways were involved in *VEGF* mRNA upregulation.

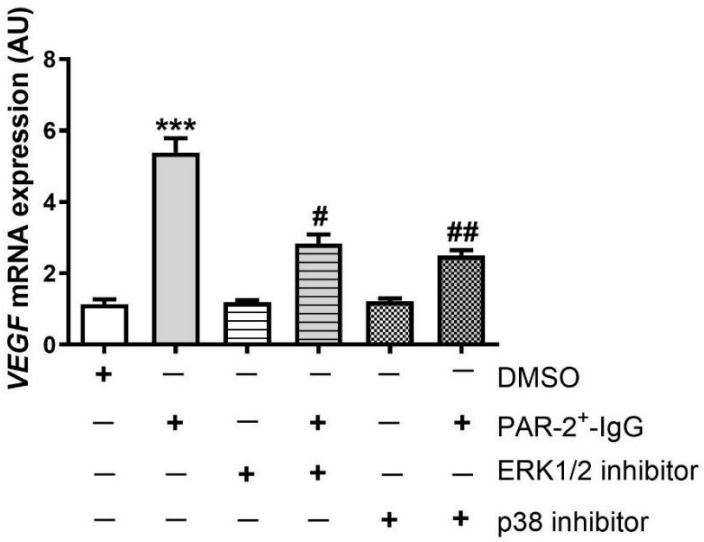

Figure 29. Effect of ERK1/2 inhibitor and p38 inhibitor on PAR-2$^+$-IgG induced *VEGF* mRNA upregulation. Cells were pre-incubated with ERK1/2 inhibitor (1.5 μM PD 184352) or p38 inhibitor (10 μM SB230580) before PAR-2$^+$-IgG stimulation. Total RNA was extracted three hours after stimulation. The *VEGF* mRNA level from DMSO treated cells was set to 1.0. Data are presented as mean ± SEM. *** $p < 0.001$ vs. con, # $p < 0.01$ vs PAR-2$^+$-IgG, ## $p < 0.001$ vs PAR-2$^+$-IgG, n=4.

4.7 Activation of *VEGF* promoter by trypsin

The previous results showed that trypsin increased the *VEGF* mRNA level. The messenger RNA level increase could have been caused by increased transcription or enhanced mRNA stability. A reporter plasmid containing the luciferase coding gene under the control of the 2.1 kb (region −2018 to +50 relative to the transcription start site) *VEGF* full-length proximal promoter was used. As shown in Figure 30, after 6 hours of stimulation, trypsin significantly increased *VEGF*-promoter luciferase activity by 14%. When PAR-2 was overexpressed by transfecting 100ng pcDNA-*PAR-2* plasmid in HMEC-1 cells, the *VEGF*-promoter luciferase activity was increased by 38% after trypsin treatment (Figure 30).

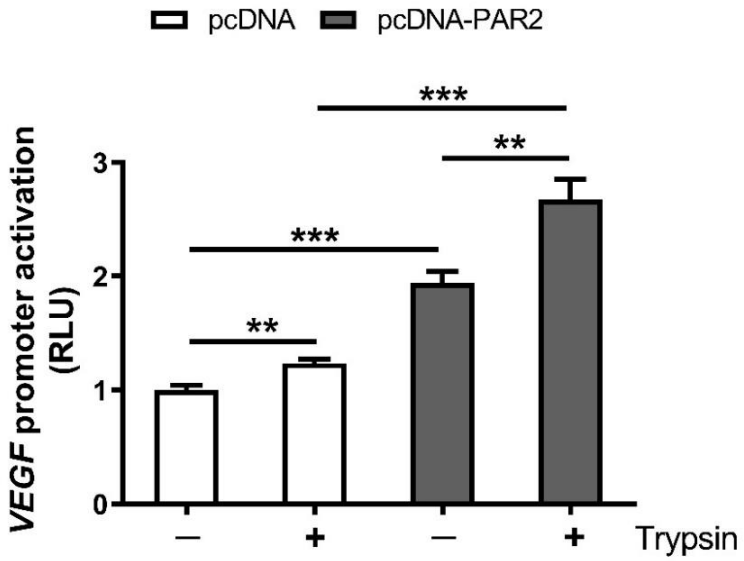

Figure 30. Effect of trypsin on *VEGF* promoter activity. Luciferase activity of the samples was calculated with the ratio firefly luciferase activity/renilla luciferase activity, the luciferase activity of pcDNA control vector was transfected, and untreated cells was set as 1.0. Data are presented as mean ± SEM. * $p < 0.05$, ** $p < 0.01$, *** $p < 0.001$, n=6.

4.8 Effect of different IgG on endothelial angiogenesis *in vitro*

PAR-2^+-IgG increased VEGF release while PAR-2^--IgG did not; whether they could differently affect angiogenesis was unknown. Matrigel angiogenesis assay was performed to investigate the effect of IgG on angiogenesis *in vitro*. As shown in Figure 31, PAR-2^+-IgG significantly increased the formation of vascular tube compared to DMEM ($p < 0.01$). Compared to PAR-2^+-IgG treated cells, cells treated with PAR-2^--IgG demonstrated impaired vascular network formation ($p < 0.05$). Though the PAR-2 blocker could slightly reduce tube formation, this effect was not significant.

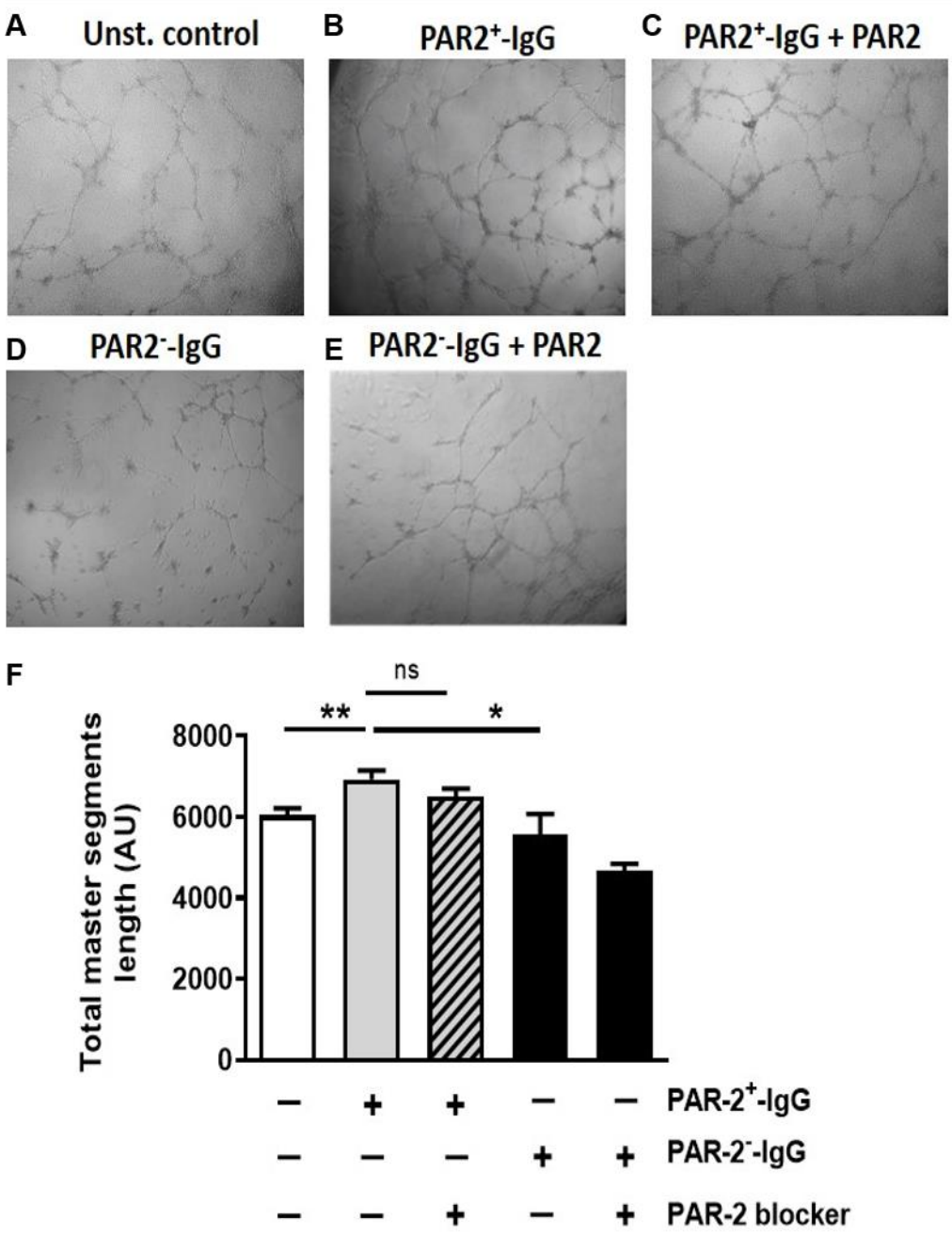

Figure 31. Effect of PAR-2^{+}-IgG and PAR-2^{-}-IgG on tube formation in an *in vitro* matrigel angiogenesis assay. A, tube formation of cells treated with DMEM low glucose medium; B, tube formation of cells treated with PAR-2^{+}-IgG; C, tube formation of cells treated with PAR-2^{+}-IgG plus PAR-2 blocker; D, tube formation of cells treated with PAR-2^{-}-IgG; E, tube formation of cells treated with PAR-2^{-}-IgG plus PAR-2 blocker; F, analysis of total master segments length of tube formation of cells using Image J Software. Data are presented as mean ± SEM. * $p < 0.05$, ** $p < 0.01$, ns, not significant, n=6.

5 Discussion

Donor endothelial cells are in direct contact with the recipient immune system and cause alloimmune responses which damage the microvasculature.(52)Angiogenesis, which is essential for renal microvascular integrity, is frequently deregulated in kidney transplant patients, leading to acute and chronic vascular rejection. Abnormal angiogenesis can cause various complications post kidney transplantation, such as impaired wound healing and proteinuria. (53, 54) Anti-GPCR autoantibodies, which are natural components of the immune system, play a role in immune homeostasis, and can trigger the development of autoimmune diseases when dysregulated.(55) PAR-2-IgG levels are dysregulated in several autoimmune diseases, and strongly correlate with the levels of autoantibodies targeting other GPCRs, growth factors and growth factor receptors in healthy individuals and patients.(55) HLA-antibodies and autoantibodies targeting GPCRs contribute to early and late graft losses; however, the role of angiogenesis-regulating autoantibodies like PAR-1 and PAR-2 haven´t been investigated to date.(56) Thus, investigating the effect of PAR-2-IgG on endothelial cells and endothelial angiogenesis is of great interest.

In this work, the function of PAR-2 and the effects of autoantibodies targeting this receptor, isolated from kidney transplant patients and healthy individuals, were investigated in the endothelial cell line HMEC-1. Results showed that in HMEC-1 PAR-2 couples with various G proteins, and its activation by natural agonist triggers the activation of multiple intracellular signaling pathways, resulting in the upregulation of VEGFA levels. Isolated PAR-2-IgG, whose levels were higher in healthy individuals compared to relatively low levels in KTx patients, upregulated the mRNA and protein levels of VEGF, and potentially contributed to the proangiogenic effect of IgG isolated from healthy individuals. Thus, PAR-2-IgG exerted both agonistic and proangiogenic activities in endothelial cells.

5.1 G-protein coupling of PAR-2

In this project, a luciferase-based reporter assay was used to investigate the G-protein signaling pathway activated by trypsin or PAR-2 AP or IgG. Using this luciferase reporter assay system, the coupling and activation of G_i or G_q, and $G_{\alpha 12}$ on PAR-2 activation by both natural ligand and

activating peptide in HMEC-1 was confirmed.

A number of other functional assay platforms have been developed for GPCR signaling pathway deciphering or GPCR target screening, including Guanine nucleotide binding assays, cAMP assays, and intracellular calcium assays.(57) The coupling of $G_{\alpha i1}$, $G_{\alpha o}$ and $G_{\alpha 12}$ was also demonstrated by M. A. Ayoubl, who applied the bioluminescence resonance energy transfer system to reveal the G protein coupling profile and β-arrestin interaction of PAR-2 in the COS7 cell line.(14) Using that real-time approach, they found that binding between G_{α} proteins and PAR-2 had different kinetics and potencies: $G_{\alpha i1}$ and $G_{\alpha o}$ coupling was ligand-independent and could be activated robustly after ligand stimulation within a few seconds, while it started to decline after 5min.(14) On the other hand, $G_{\alpha 12}$ coupling completely depended on agonist stimulation and required a longer time for full activation (around 30 min).(14)

Using both ectopic cellular systems expressing recombinant proteins (COS-7 kidney cells lacking functional PAR measures) and cells of neuronal origin that natively express PARs (Neu7 astroglia), Kelly L. McCoy showed that PAR-2 couples to $G_{q/11}$ family members (G_q, G_{11}, and G_{14}), $G_{\alpha 12/13}$ family members ($G_{\alpha 12}$ and G_{13}), and to the downstream signaling pathways activated by these G proteins.(15)

Using the luciferase reporter assay and western blot, the activation of ERK1/2, which could have resulted from G_i, G_q or β-arrestin activation, was shown. One limitation of this work was that the coupling between PAR-2 and β-arrestins was not investigated. β-arrestin-mediated ERK1/2 activation leads to distinct signaling pathway and cellular function changes. β-arrestin-dependent endocytosis of PAR-2 leads to the activation of cytosolic-retained ERK1/2, which neither translocates to the nucleus nor causes cell proliferation.(58) In comparison, mutant PAR-2, which does not interact with β-arrestin 1, causes ERK1/2 nucleus translocation and cell proliferation when activated. In MDA MB-231 breast cancer cells, β-arrestin 1 and 2 mediated ERK1/2 was indispensable for PAR-2 mediated cancer cell migration.(59) Prolonged ERK1/2 activation mediated by β-arrestin-dependent scaffolding complex was retained at the plasma membrane and was critical for PAR-2-induced chemotaxis in pseudopodia.(60) Here, in terms of HMEC-1, although a prolonged ERK1/2 activation was not seen, it will be interesting to investigate the contribution of β-arrestin to trypsin-induced signaling in the future.

5.2 PAR-2 and VEGF/VEGFR signaling

Various GPCRs have recently emerged as key regulators of survival, growth, angiogenesis and metastasis of tumor, which is due to the cross-talk between these GPCRs and the VEGF/VEGFR system.(61) According to the results of this work, trypsin and PAR-2^{+}-IgG stimulation could increase the *VEGF* mRNA level and VEGF protein secretion.

Findings from other researchers show that PAR-2 activation can upregulate the expression of VEGFA and is proangiogenic both *in vivo* and *in vitro*. PAR-2 promotes retinal neovascularization through inducing tumor necrosis factor-alpha (TNF-α).(62) PAR-2, abundantly expressing in retinal ganglion cells, is associated with new blood vessel formation during retinal development, and in ischemic retinopathy in mice.(63) Injection of trypsin or PAR-2 AP improves hemodynamic recovery and enhances limb salvage, due to the enhancement of reparative angiogenesis in mice, demonstrating the proangiogenic effect of PAR-2 stimulation *in vivo*.(64)

The results showed that trypsin stimulation led to p38, ERK1/2, and PI3K/Akt signaling pathway activation. Activation of these signaling pathways may account for VEGF production induced by trypsin treatment. Y. Liu reported that PAR-2 AP, trypsin or tissue factor (factor VIIa) treatment could result in a robust increase in *VEGF* mRNA and protein levels via ERK1/2 and p38 pathways in the MDA-MB-231 cells.(65) In pancreatic cancer cells, activated PAR-2 enhances tumor angiogenesis through the induction of the synthesis of VEGFA via the ERK1/2 pathway, independent of HIF1-α pathways.(66) The PAR-2/MAPK signaling axis, but not the PI3K/Akt pathway, accounted for the induction of VEGF production in two human glioblastoma cell lines, A172 and U87-MG.(67) However, in human adipose stem cells, both MEK/ERK and PI3-kinase/Akt pathway activation were involved in the induction of VEGF secretion evoked by trypsin stimulation.(68) It will be interesting to investigate the contribution of these pathways to VEGF protein secretion in HMEC-1 in the future.

One finding from this work was that trypsin greatly increased the *VEGF* mRNA and protein levels, but only slightly increased the transcription activity of 2.1kb *VEGF* gene proximal promoter. The transcription of the *VEGF* mRNA is regulated by several transcription factors, including activator protein 1, HIF-1 α, specificity protein 1, and β-catenin.(69) In HEK293 cells, nuclear PAR-2 recruited Sp1 to bind the *VEGF* promoter and induced the transcription of *VEGF*.(63) In BxPC-3,

a pancreatic cancer cell line, HIF-1 α and HIF-2 α were not responsible for the induction of VEGF, although their protein level was upregulated by PAR-2 AP or tissue factor-factor VIIa treatment.(66) PAR-2 activation may elevate the *VEGF* mRNA level via mRNA stabilization without altering *VEGF* gene transcription in certain cell types. PAR-2 may increase *VEGF* mRNA, via downregulating microRNAs (miRNA) that degrade *VEGF* mRNA. PAR-2 activation downregulated the level of miRNA-34a in colonic cancer cells.(70) MiR-34a exerted an anti-tumor effect in colorectal cancer via inhibiting VEGF expression *in vivo*.(71) Further work needs to be done to investigate the mechanism of *VEGF* mRNA induction by trypsin in endothelial cells.

5.3 Agonistic and proangiogenic PAR-2-IgG

Antiendothelial cell antibodies (AECA) have been identified and shown to be abnormally elevated in a variety of human diseases, including SSc, systemic lupus erythematosus and idiopathic pulmonary fibrosis.(72-74) AECA in SSc patients induce the apoptosis of endothelial cells and lead to vascular injury.(75, 76) These AECA may be pathogenic and can serve as an important marker for disease severity. The effect of AECA (including autoantibodies directed against GPCRs) on inflammation and fibrosis has been extensively studied; their effect (especially autoantibodies targeting GPCRs) on vascular angiogenesis, which is also dysregulated in various human diseases and in patients after organ transplantation, has been studied less.(33, 77-80)

The work in this thesis studied the effect of PAR-2-IgG on endothelial angiogenesis. The results show that PAR-2-IgG partially contributed to the increased VEGF release induced by IgG isolated from healthy individuals. As trypsin, a PAR-2 natural agonist, increased VEGF production in HMEC-1 cells, PAR-2-IgG acted as agonistic autoantibodies and were proangiogenic.

The result that PAR-2-IgG was proangiogenic might be consistent with an exploratory study by Kjartan Moe *et al*.(81) Their work showed that preeclamptic pregnancies had lower levels of autoantibodies against PAR-1, PAR-2, VEGF, VEGFB, PlGF, VEGFR-1 and VEGFR-2 than normotensive pregnancies. Clinical features associated with augmented risk for the preeclampsia syndrome were associated with lower levels of the autoantibodies, indicating a protective role of these autoantibodies in the development of preeclampsia.(81) As preeclampsia is caused by

deficient angiogenesis, autoantibodies targeting PAR-2 may promote angiogenesis.(82)

The PAR-2-IgG investigated in this study were proangiogenic; autoantibodies targeting other GPCRs can also influence angiogenesis, being either proangiogenic or anti-angiogenic. Autoantibodies against muscarinic acetylcholine receptors (mAchR) can be detected in the sera of breast cancer patients.(83) Purified IgG from breast cancer patients in T1N0Mx stage stimulates the secretion of VEGF and increases tumor neovascularization.(83) These effects can be significantly blocked by atropine, a muscarinic antagonist, demonstrating the participation of mAchR autoantibodies in tumor vascular angiogenesis.(83) A recent study shows that AT_1R IgG can enhance the migration of ovarian cancer cells, and AT_1R IgG-treated chorioallantoic membrane shows increased vascular density, indicating the proangiogenic effect of AT_1R IgG.(84) But autoantibody-mediated complement C3a receptor (C3aR) is anti-angiogenic. Activation of C3aR by C3aR IgG induces the release of sVEGFR-1 and decreases angiogenesis.(85) AT_1R IgG in preeclamptic women can induce the secretion of soluble endoglin, sVEGFR-1, and endothelin 1.(32) sVEGFR-1 antagonizes membrane VEGFR-mediated signaling, causing hypertension and renal dysfunction.(32) Soluble endoglin inhibited VEGF mediated capillary tube formation *in vitro* and induced vascular permeability *in vivo* in vasculature.(82) Therefore, AT_1R IgG contributes to the anti-angiogenic state, which is characteristic of preeclampsia.

Although the autoantibodies targeting PAR-2 detected here were agonistic, the possibility of the presence of antagonistic or neutralizing autoantibodies against PAR-2 could not be excluded. Autoantibodies directed against GPCR are biased ligands for the receptor, they may bind to the receptor, trigger different signaling pathways and induce different cellular responses, that differ from the natural ligands. For example, human monoclonal autoantibody M22 is a thyroid-stimulating autoantibody, whereas another TSHR monoclonal antibody CS-17 reduces the constitutive cAMP activity induced by TSHR overexpression in COS-7 cells and suppresses gain-of-function TSHR mutations, displaying inverse agonist activity.(86) Both agonistic and antagonistic autoantibodies directed against M3-muscarinic receptors have been characterized in Sjögren's syndrome patients.(87) The different action of these autoantibodies is probably due to the difference in the extracellular domains that the antibodies recognized.(87) Autoantibodies recognizing the B cell epitopes within the second ECL inhibited the increase of calcium induced

by cevimeline, a muscarinic agonist, whereas autoantibodies recognizing B cell epitopes within the N terminal loop or the first ECL induced intracellular calcium influx.(87) Autoantibodies to the third ECL had no effect on calcium influx.(87)

5.4 Reduced PAR-2-IgG level and dysregulated angiogenesis after kidney transplant

In this work, the level of PAR-2-IgG in healthy subjects and kidney transplant patients was measured, and the effect of IgG on endothelial VEGF secretion was also investigated. The PAR-2-IgG ELISA result showed that the PAR-2-IgG level was relatively lower in kidney transplant patients compared to healthy individuals, and VEGF ELISA showed that IgG from healthy subjects increased endothelial VEGF secretion, while IgG from KTx patients did not. Though the exact reason for this phenomenon was unknown, the use of immune-suppressive drug therapy after kidney transplants may account for that.

Kidney transplantation provides a higher quality of life, a better survival, and a lower morbidity for ESRD patients than hemodialysis or peritoneal dialysis treatment do.(88) In order to modulate the response of transplant recipient's immune system to the donor organ, lifelong immunosuppressive agents are administered to the recipients.(89) Immunosuppressive agents, including intravenous immunoglobulin, anti-CD20 monoclonal antibody, and Campath-1H compromise the immune system and reduce the production of antidonor antibodies post-transplantation.(90) These immunosuppressive drugs may also reduce the generation of autoantibodies directed against GPCR, including PAR-2-IgG.

VEGF signaling is related to both acute and chronic renal allograft rejection, as well as the development of various complications. Higher VEGF production, encoded by *−1154*G* and *−2578*C* containing genotypes, is strongly associated with acute renal allograft rejection.(91) A markedly increased expression of Fractalkine and VEGF protein can be detected in the interstitium of chronic rejection patients compared with non-chronic rejection patients, indicating a role for them in chronic renal allograft rejection.(92) The use of immune-suppressive drug therapy post kidney transplantation has been shown to lead to undesired consequences of immunodeficiency, like wound healing complications, increased cancer incidence and proteinuria. Those

complications are caused by dysregulated vascular angiogenesis.

The use of rapamycin (sirolimus) as immunosuppressant after kidney transplantation has been associated with an increased risk of wound-healing complications.(54) The inhibition of VEGFA function and nitric oxide by sirolimus contributes to impaired would healing.(93) Proteinuria, a dose-related side effect due to the inhibition of VEGF signaling, is a common complication caused by long-term immunosuppressive drug usage.(53) VEGF121 treatment ameliorates the development of hypertension and nephropathy caused by the administration of cyclosporine A (CsA) in mice.(94) The overall incidence of cancer is markedly increased after kidney transplantation.(3) Immunosuppressive drug therapy after renal transplantation is thought to be the main cause of increased cancer incidence.(3) Different immunosuppressive drugs have differing effects on VEGFA signaling, thus they affect cancer incidence differently after transplantation. CsA treatment increases the risk of cancer via directly promoting the production of VEGFA and inducing the growth of established cancer cells.(95) In contrast to CsA, rapamycin has a potent anti-cancer effect and can reduce the occurrence of cancer after kidney transplantation due to its inhibitory effect on VEGF production and VEGF signaling.(96) Switching to sirolimus-based therapy after CsA withdrawal at month 3 significantly reduced the risk for both skin and non-skin malignancies at 5 years after renal transplantation.(97) Thus, the inability of IgG from KTx patients to induce endothelial VEGF production and reduced proangiogenic PAR-2-IgG may contribute to the impaired VEGF signaling and development of complications post kidney transplant.

5.5 Perspective

In the present work, the presence of autoantibodies targeting PAR-2 was detected in both healthy individuals and kidney transplant patients. Kidney transplant patients had lower PAR-2-IgG levels than healthy individuals. PAR-2-IgG present in healthy individuals were shown to be agonistic and proangiogenic. Furthermore, total IgG from healthy individuals increased VEGF protein level, while total IgG from kidney transplant patients did not. Future work could focus on the following aspects:

1) A large cohort study investigating a correlation of PAR-1 levels and cancer development in kidney transplant patients showed that low PAR-1 antibody levels were associated with higher

cancer incidence and lower angiogenic potency *in vitro.*(6) Whether low PAR-2 antibody levels in transplant patients have a similar correlation or not still has to be investigated, as well as distinctive cut-off values.

2) Investigating epitopes recognized by PAR-2-IgG. The majority of the functional autoantibodies against GPCR recognize the extracellular loop of the GPCR. For example, AT_1R IgG recognized two epitopes located within the ECL2 of the AT_1R.(5) Affinity-purified antibodies to the amino-terminal portion of ECL2 transiently increased intracellular free Ca^{2+} concentration and were agonistic.(98) Characterizing the epitopes could give insight into the activating mechanism of the receptor by PAR-2-IgG.
3) Analyzing the level of PAR-2-IgG in human diseases, and its correlation with disease progression. PAR-2 level is elevated in various diseases, and activation of PAR-2 leads to disease development and progression. As mentioned previously, the level of autoantibodies directed against GPCR may be used as a prognostic marker in certain diseases. Agonistic PAR-2-IgG might be of prognostic value for certain diseases, like preeclampsia syndrome, cancer, diabetic nephropathy, and systemic sclerosis. Indeed, an increased PAR-2-IgG level has been detected in patients with systemic lupus erythematosus and systemic sclerosis, while reduced PAR-2-IgG level was detected in patients with the disease of granulomatosis with polyangiitis.(55) But the value of the PAR-2-IgG level as disease biomarker needs further investigation.

6 References

1. Garcia GG, Harden P, Chapman J. The global role of kidney transplantation. Kidney and Blood Pressure Research. 2012;35:299-304.
2. Puttarajappa C, Shapiro R, Tan HP. Antibody-mediated rejection in kidney transplantation: a review. Journal of transplantation. 2012;2012.
3. Vajdic CM, McDonald SP, McCredie MR, Van Leeuwen MT, Stewart JH, Law M, Chapman JR, Webster AC, Kaldor JM, Grulich AE. Cancer incidence before and after kidney transplantation. Jama. 2006;296:2823-31.
4. Xia Y, Kellems RE. Receptor-activating autoantibodies and disease: preeclampsia and beyond. Expert review of clinical immunology. 2011;7:659-74.
5. Dragun D, Müller DN, Bräsen JH, Fritsche L, Nieminen-Kelhä M, Dechend R, Kintscher U, Rudolph B, Hoebeke J, Eckert D. Angiotensin II type 1–receptor activating antibodies in renal-allograft rejection. New England Journal of Medicine. 2005;352:558-69.
6. Catar R, Carroll R, Schramm I, Simon M, Wischnewski O, Kusch A, Coates T, Philippe A, Dragun D. Loss of regulatory anti-angiogenic Protease-activated receptor-1 (PAR-1) antibodies associate with the development of metastatic cancer post renal transplantation and patient death. Transplant international; 2016.
7. Camerer E, Huang W, Coughlin SR. Tissue factor-and factor X-dependent activation of protease-activated receptor 2 by factor VIIa. Proceedings of the National Academy of Sciences. 2000;97:5255-60.
8. Kahn ML, Hammes SR, Botka C, Coughlin SR. Gene and locus structure and chromosomal localization of the protease-activated receptor gene family. Journal of Biological Chemistry. 1998;273:23290-6.
9. Steven J, Sandhu S, Wijesuriya SJ, Hollenberg MD. Glycosylation of human proteinase-activated receptor-2 (hPAR2): role in cell surface expression and signalling. Biochemical Journal. 2002;368:495-505.
10. R. D'Andrea M, Derian CK, Leturcq D, Baker SM, Brunmark A, Ling P, Darrow AL, Santulli RJ, Brass LF, Andrade–Gordon P. Characterization of protease-activated receptor-2 immunoreactivity in normal human tissues. Journal of Histochemistry & Cytochemistry. 1998;46:157-64.
11. Molino M, Barnathan ES, Numerof R, Clark J, Dreyer M, Cumashi A, Hoxie JA, Schechter N, Woolkalis M, Brass LF. Interactions of mast cell tryptase with thrombin receptors and PAR-2. Journal of Biological Chemistry. 1997;272:4043-9.
12. Al‐Ani B, Saifeddine M, Kawabata A, Hollenberg MD. Proteinase activated receptor 2: role of extracellular loop 2 for ligand‐mediated activation. British journal of pharmacology. 1999;128:1105-13.
13. Ungefroren H, Witte D, Rauch B, Settmacher U, Lehnert H, Gieseler F, Kaufmann R. Proteinase-Activated Receptor 2 May Drive Cancer Progression by Facilitating TGF-β Signaling. International journal of molecular sciences. 2017;18:2494.
14. Ayoub MA, Pin J-PR. Interaction of protease-activated receptor 2 with G proteins and β-arrestin 1 studied by bioluminescence resonance energy transfer. Frontiers in endocrinology. 2013;4:196.
15. McCoy KL, Traynelis SF, Hepler JR. PAR1 and PAR2 couple to overlapping and distinct sets of G proteins and linked signaling pathways to differentially regulate cell physiology. Molecular pharmacology. 2010;77:1005-15.
16. Stalheim L, Ding Y, Gullapalli A, Paing MM, Wolfe BL, Morris DR, Trejo J. Multiple independent functions of arrestins in the regulation of protease-activated receptor-2 signaling and trafficking. Molecular pharmacology. 2005;67:78-87.
17. Jiang Y, Yau M-K, Kok WM, Lim J, Wu K-C, Liu L, Hill TA, Suen JY, Fairlie DP. Biased signaling by agonists of Protease-activated receptor 2. ACS chemical biology. 2017;12:1217-26.
18. Rothmeier AS, Ruf W, editors. Protease-activated receptor 2 signaling in inflammation. Seminars in immunopathology; 2012: Springer.

19. Grandaliano G, Pontrelli P, Cerullo G, Monno R, Ranieri E, Ursi M, Loverre A, Gesualdo L, Schena FP. Protease-activated receptor-2 expression in IgA nephropathy: a potential role in the pathogenesis of interstitial fibrosis. Journal of the American Society of Nephrology. 2003;14:2072-83.
20. Wygrecka M, Kwapiszewska G, Jablonska E, Gerlach Sv, Henneke I, Zakrzewicz D, Guenther A, Preissner KT, Markart P. Role of protease-activated receptor-2 in idiopathic pulmonary fibrosis. American journal of respiratory and critical care medicine. 2011;183:1703-14.
21. Morris DR, Ding Y, Ricks TK, Gullapalli A, Wolfe BL, Trejo J. Protease-activated receptor-2 is essential for factor viia and xa–induced signaling, migration, and invasion of breast cancer cells. Cancer research. 2006;66:307-14.
22. Hara T, Phuong PT, Fukuda D, Yamaguchi K, Murata C, Nishimoto S, Yagi S, Kusunose K, Yamada H, Soeki T. Protease-Activated Receptor-2 Plays a Critical Role in Vascular Inflammation and Atherosclerosis in Apolipoprotein E–Deficient Mice. Circulation. 2018;138:1706-19.
23. Antoniak S, Sparkenbaugh EM, Tencati M, Rojas M, Mackman N, Pawlinski R. Protease-activated receptor-2 contributes to heart failure. PLoS One. 2013;8:e81733.
24. Coutinho A, Kazatchkine MD, Avrameas S. Natural autoantibodies. Current opinion in immunology. 1995;7:812-8.
25. Nagele EP, Han M, Acharya NK, DeMarshall C, Kosciuk MC, Nagele RG. Natural IgG autoantibodies are abundant and ubiquitous in human sera, and their number is influenced by age, gender, and disease. PLoS One. 2013;8:e60726.
26. Kroeze WK, Sheffler DJ, Roth BL. G-protein-coupled receptors at a glance. Journal of cell science. 2003;116:4867-9.
27. Costagliola S, Many M-C, Denef J-F, Pohlenz J, Refetoff S, Vassart G. Genetic immunization of outbred mice with thyrotropin receptor cDNA provides a model of Graves' disease. The Journal of clinical investigation. 2000;105:803-11.
28. Nagayama Y, Kita-Furuyama M, Ando T, Nakao K, Mizuguchi H, Hayakawa T, Eguchi K, Niwa M. A novel murine model of Graves' hyperthyroidism with intramuscular injection of adenovirus expressing the thyrotropin receptor. The Journal of Immunology. 2002;168:2789-94.
29. Jahns R, Boivin V, Lohse MJ. β1-adrenergic receptor function, autoimmunity, and pathogenesis of dilated cardiomyopathy. Trends in cardiovascular medicine. 2006;16:20-4.
30. Zhou Z, Liao Y-H, Wei Y, Wei F, Wang B, Li L, Wang M, Liu K. Cardiac remodeling after long-term stimulation by antibodies against the α1-adrenergic receptor in rats. Clinical Immunology. 2005;114:164-73.
31. Wenzel K, Haase H, Wallukat G, Derer W, Bartel S, Homuth V, Herse F, Hubner N, Schulz H, Janczikowski M. Potential relevance of α1-adrenergic receptor autoantibodies in refractory hypertension. PloS one. 2008;3:e3742.
32. Xia Y, Kellems RE. Angiotensin receptor agonistic autoantibodies and hypertension: preeclampsia and beyond. Circulation research. 2013;113:78-87.
33. Riemekasten G, Philippe A, Näther M, Slowinski T, Müller DN, Heidecke H, Matucci-Cerinic M, Czirják L, Lukitsch I, Becker M. Involvement of functional autoantibodies against vascular receptors in systemic sclerosis. Annals of the rheumatic diseases. 2011;70:530-6.
34. Buschmann I, Schaper W. Arteriogenesis versus angiogenesis: two mechanisms of vessel growth. Physiology. 1999;14:121-5.
35. Risau W. Mechanisms of angiogenesis. nature. 1997;386:671.
36. Carmeliet P, Ferreira V, Breier G, Pollefeyt S, Kieckens L, Gertsenstein M, Fahrig M, Vandenhoeck A, Harpal K, Eberhardt C. Abnormal blood vessel development and lethality in embryos lacking a single VEGF allele. Nature. 1996;380:435.
37. Nagy JA, Vasile E, Feng D, Sundberg C, Brown LF, Detmar MJ, Lawitts JA, Benjamin L, Tan X, Manseau EJ.

Vascular permeability factor/vascular endothelial growth factor induces lymphangiogenesis as well as angiogenesis. Journal of Experimental Medicine. 2002;196:1497-506.
38. Chung AS, Lee J, Ferrara N. Targeting the tumour vasculature: insights from physiological angiogenesis. Nature Reviews Cancer. 2010;10:505.
39. Wei M-H, Popescu NC, Zimonjic D, Lerman M, Merrill M. Localization of the human vascular endothelial growth factor gene, VEGF, at chromosome 6p12. Human genetics. 1996;97:794-7.
40. Enomoto H, Inoki I, Komiya K, Shiomi T, Ikeda E, Obata K-i, Matsumoto H, Toyama Y, Okada Y. Vascular endothelial growth factor isoforms and their receptors are expressed in human osteoarthritic cartilage. The American journal of pathology. 2003;162:171-81.
41. Ratcliffe PJ. HIF-1 and HIF-2: working alone or together in hypoxia? The Journal of clinical investigation. 2007;117:862-5.
42. Ferrara N, Gerber H-P, LeCouter J. The biology of VEGF and its receptors. Nature medicine. 2003;9:669.
43. Ferrara N, Davis-Smyth T. The biology of vascular endothelial growth factor. Endocrine reviews. 1997;18:4-25.
44. Barleon B, Sozzani S, Zhou D, Weich HA, Mantovani A, Marme D. Migration of human monocytes in response to vascular endothelial growth factor (VEGF) is mediated via the VEGF receptor flt-1. Blood. 1996;87:3336-43.
45. Fiedler J, Leucht F, Waltenberger J, Dehio C, Brenner RE. VEGF-A and PlGF-1 stimulate chemotactic migration of human mesenchymal progenitor cells. Biochemical and biophysical research communications. 2005;334:561-8.
46. Gabrilovich DI, Chen HL, Girgis KR, Cunningham HT, Meny GM, Nadaf S, Kavanaugh D, Carbone DP. Production of vascular endothelial growth factor by human tumors inhibits the functional maturation of dendritic cells. Nature medicine. 1996;2:1096.
47. Maynard SE, Min J-Y, Merchan J, Lim K-H, Li J, Mondal S, Libermann TA, Morgan JP, Sellke FW, Stillman IE. Excess placental soluble fms-like tyrosine kinase 1 (sFlt1) may contribute to endothelial dysfunction, hypertension, and proteinuria in preeclampsia. The Journal of clinical investigation. 2003;111:649-58.
48. Aiello LP, Pierce EA, Foley ED, Takagi H, Chen H, Riddle L, Ferrara N, King GL, Smith L. Suppression of retinal neovascularization in vivo by inhibition of vascular endothelial growth factor (VEGF) using soluble VEGF-receptor chimeric proteins. Proceedings of the National Academy of Sciences. 1995;92:10457-61.
49. Ferrara N, Hillan KJ, Novotny W. Bevacizumab (Avastin), a humanized anti-VEGF monoclonal antibody for cancer therapy. Biochemical and biophysical research communications. 2005;333:328-35.
50. Genomics-online. Mammalian expression vector pcDNA3.1 with the CMV promoter [Available from: https://www.genomics-online.com/vector-backbone/55/pcdna3.1/.
51. Cheng Z, Garvin D, Paguio A, Stecha P, Wood K, Fan F. Luciferase reporter assay system for deciphering GPCR pathways. Current chemical genomics. 2010;4:84.
52. Valenzuela NM, Reed EF. Antibody-mediated rejection across solid organ transplants: manifestations, mechanisms, and therapies. The Journal of clinical investigation. 2017;127:2492-504.
53. Letavernier E, Legendre C. mToR inhibitors-induced proteinuria: mechanisms, significance, and management. Transplantation Reviews. 2008;22:125-30.
54. Dean PG, Lund WJ, Larson TS, Prieto M, Nyberg SL, Ishitani MB, Kremers WK, Stegall MD. Wound-healing complications after kidney transplantation: a prospective, randomized comparison of Sirolimus and Tacrolimus1. Transplantation. 2004;77:1555-61.
55. Cabral-Marques O, Marques A, Giil LM, De Vito R, Rademacher J, Günther J, Lange T, Humrich JY, Klapa S, Schinke S. GPCR-specific autoantibody signatures are associated with physiological and pathological immune homeostasis. Nature communications. 2018;9:5224.
56. Dragun D, Catar R, Philippe A. Non-HLA antibodies in solid organ transplantation: recent concepts and clinical relevance. Current opinion in organ transplantation. 2013;18:430-5.

57. Thomsen W, Frazer J, Unett D. Functional assays for screening GPCR targets. Current opinion in biotechnology. 2005;16:655-65.
58. DeFea K, Zalevsky J, Thoma M, Dery O, Mullins R, Bunnett N. β-Arrestin–dependent endocytosis of proteinase-activated receptor 2 is required for intracellular targeting of activated ERK1/2. The Journal of cell biology. 2000;148:1267-82.
59. Ge L, Shenoy SK, Lefkowitz RJ, DeFea K. Constitutive protease-activated receptor-2-mediated migration of MDA MB-231 breast cancer cells requires both β-arrestin-1 and-2. Journal of Biological Chemistry. 2004;279:55419-24.
60. Ge L, Ly Y, Hollenberg M, DeFea K. A β-arrestin-dependent scaffold is associated with prolonged MAPK activation in pseudopodia during protease-activated receptor-2-induced chemotaxis. Journal of Biological Chemistry. 2003;278:34418-26.
61. Dorsam RT, Gutkind JS. G-protein-coupled receptors and cancer. Nature reviews cancer. 2007;7:79.
62. Zhu T, Sennlaub F, Beauchamp MH, Fan L, Joyal JS, Checchin D, Nim S, Lachapelle P, Sirinyan M, Hou X. Proangiogenic effects of protease-activated receptor 2 are tumor necrosis factor-α and consecutively Tie2 dependent. Arteriosclerosis, thrombosis, and vascular biology. 2006;26:744-50.
63. Joyal J-S, Nim S, Zhu T, Sitaras N, Rivera JC, Shao Z, Sapieha P, Hamel D, Sanchez M, Zaniolo K. Subcellular localization of coagulation factor II receptor-like 1 in neurons governs angiogenesis. Nature medicine. 2014;20:1165.
64. Milia AF, Salis MB, Stacca T, Pinna A, Madeddu P, Trevisani M, Geppetti P, Emanueli C. Protease-activated receptor-2 stimulates angiogenesis and accelerates hemodynamic recovery in a mouse model of hindlimb ischemia. Circulation research. 2002;91:346-52.
65. Liu Y, Mueller BM. Protease-activated receptor-2 regulates vascular endothelial growth factor expression in MDA-MB-231 cells via MAPK pathways. Biochemical and biophysical research communications. 2006;344:1263-70.
66. Chang L-H, Pan S-L, Lai C-Y, Tsai A-C, Teng C-M. Activated PAR-2 regulates pancreatic cancer progression through ILK/HIF-α–induced TGF-α expression and MEK/VEGF-A–mediated angiogenesis. The American journal of pathology. 2013;183:566-75.
67. Dutra-Oliveira A, Monteiro RQ, Mariano-Oliveira A. Protease-activated receptor-2 (PAR2) mediates VEGF production through the ERK1/2 pathway in human glioblastoma cell lines. Biochemical and biophysical research communications. 2012;421:221-7.
68. Rasmussen JG, Riis SE, Frøbert O, Yang S, Kastrup J, Zachar V, Simonsen U, Fink T. Activation of protease-activated receptor 2 induces VEGF independently of HIF-1. Plos one. 2012;7:e46087.
69. Birk DM, Barbato J, Mureebe L, Chaer RA. Basic science review: current insights on the biology and clinical aspects of VEGF regulation. Vascular and endovascular surgery. 2009;42:517-30.
70. Ma Y, Bao-Han W, Lv X, Su Y, Zhao X, Yin Y, Zhang X, Zhou Z, MacNaughton WK, Wang H. MicroRNA-34a mediates the autocrine signaling of PAR2-activating proteinase and its role in colonic cancer cell proliferation. PloS one. 2013;8:e72383.
71. Zhang D, Qiu X, Li J, Zheng S, Li L, Zhao H. TGF-β secreted by tumor-associated macrophages promotes proliferation and invasion of colorectal cancer via miR-34a-VEGF axis. Cell Cycle. 2018;17:2766-78.
72. Salojin KV, Saraux A, Nassonov EL, Dueymes M, Piette J-C, Youinou PY. Antiendothelial cell antibodies: useful markers of systemic sclerosis. The American journal of medicine. 1997;102:178-85.
73. Yoshio T, Masuyama J, Sumiya M, Minota S, Kano S. Antiendothelial cell antibodies and their relation to pulmonary hypertension in systemic lupus erythematosus. The Journal of rheumatology. 1994;21:2058-63.
74. Magro CM, Waldman WJ, Knight DA, Allen JN, Nadasdy T, Frambach GE, Ross P, Marsh CB. Idiopathic pulmonary fibrosis related to endothelial injury and antiendothelial cell antibodies. Human immunology. 2006;67:284-

97.
75. Bordron A, Dueymes M, Levy Y, Jamin C, Leroy J-P, Piette J-C, Shoenfeld Y, Youinou PY. The binding of some human antiendothelial cell antibodies induces endothelial cell apoptosis. The Journal of clinical investigation. 1998;101:2029-35.
76. Pignone A, Scaletti C, Matucci-Cerinic M, Vazquez-Abad D, Meroni P, Del NP, Falcini F, Generini S, Rothfield N, Cagnoni M. Anti-endothelial cell antibodies in systemic sclerosis: significant association with vascular involvement and alveolo-capillary impairment. Clinical and experimental rheumatology. 1998;16:527-32.
77. Distler O, Distler JrH, Scheid A, Acker T, Hirth A, Rethage J, Michel BA, Gay RE, Müller-Ladner U, Matucci-Cerinic M. Uncontrolled expression of vascular endothelial growth factor and its receptors leads to insufficient skin angiogenesis in patients with systemic sclerosis. Circulation research. 2004;95:109-16.
78. Cosgrove GP, Brown KK, Schiemann WP, Serls AE, Parr JE, Geraci MW, Schwarz MI, Cool CD, Worthen GS. Pigment epithelium–derived factor in idiopathic pulmonary fibrosis: a role in aberrant angiogenesis. American journal of respiratory and critical care medicine. 2004;170:242-51.
79. Navarro C, Candia-Zuniga L, Silveira L, Ruiz V, Gaxiola M, Avila M, Amigo M. Vascular endothelial growth factor plasma levels in patients with systemic lupus erythematosus and primary antiphospholipid syndrome. Lupus. 2002;11:21-4.
80. Günther J, Kill A, Becker MO, Heidecke H, Rademacher J, Siegert E, Radić M, Burmester G-R, Dragun D, Riemekasten G. Angiotensin receptor type 1 and endothelin receptor type A on immune cells mediate migration and the expression of IL-8 and CCL18 when stimulated by autoantibodies from systemic sclerosis patients. Arthritis research & therapy. 2014;16:R65.
81. Moe K, Heidecke H, Dechend R, Staff AC. P46. Dysregulated level of novel circulating autoantibodies in preeclampsia. Pregnancy Hypertension: An International Journal of Women's Cardiovascular Health. 2015;5:247-8.
82. Levine RJ, Lam C, Qian C, Yu KF, Maynard SE, Sachs BP, Sibai BM, Epstein FH, Romero R, Thadhani R. Soluble endoglin and other circulating antiangiogenic factors in preeclampsia. New England Journal of Medicine. 2006;355:992-1005.
83. Lombardi MG, Negroni MP, Pelegrina LT, Castro ME, Fiszman GL, Azar ME, Morgado CC, Sales ME. Autoantibodies against muscarinic receptors in breast cancer: their role in tumor angiogenesis. PloS one. 2013;8:e57572.
84. Song L, Zhang S-L, Bai K-H, Yang J, Xiong H-Y, Li X, Liu T, Liu H-R. Serum agonistic autoantibodies against type-1 angiotensin II receptor titer in patients with epithelial ovarian cancer: a potential role in tumor cell migration and angiogenesis. Journal of ovarian research. 2013;6:22.
85. Wang W, Irani RA, Zhang Y, Ramin SM, Blackwell SC, Tao L, Kellems RE, Xia Y. Autoantibody-mediated complement C3a receptor activation contributes to the pathogenesis of preeclampsia. Hypertension. 2012;60:712-21.
86. Chen C-R, McLachlan SM, Rapoport B. Suppression of thyrotropin receptor constitutive activity by a monoclonal antibody with inverse agonist activity. Endocrinology. 2007;148:2375-82.
87. Tsuboi H, Matsumoto I, Wakamatsu E, Nakamura Y, Iizuka M, Hayashi T, Goto D, Ito S, Sumida T. New epitopes and function of anti‐M3 muscarinic acetylcholine receptor antibodies in patients with Sjögren's syndrome. Clinical & Experimental Immunology. 2010;162:53-61.
88. O'Shaughnessy MM, Montez-Rath ME, Lafayette RA, Winkelmayer WC. Differences in initial treatment modality for end-stage renal disease among glomerulonephritis subtypes in the USA. Nephrology Dialysis Transplantation. 2015;31:290-8.
89. Holt CD. Overview of Immunosuppressive Therapy in Solid Organ Transplantation. Anesthesiology clinics. 2017;35:365-80.
90. Cruzado JM, Bestard O, Grinyo JM. Control of anti-donor antibody production post-transplantation:

conventional and novel immunosuppressive therapies. Humoral Immunity in Kidney Transplantation. 162: Karger Publishers; 2009. p. 117-28.
91. Shahbazi M, Fryer AA, Pravica V, Brogan IJ, Ramsay HM, Hutchinson IV, Harden PN. Vascular endothelial growth factor gene polymorphisms are associated with acute renal allograft rejection. Journal of the American Society of Nephrology. 2002;13:260-4.
92. Cao G, Lu Y, Gao R, Xin Y, Teng D, Wang J, Li Y, editors. Expression of fractalkine, CX3CR1, and vascular endothelial growth factor in human chronic renal allograft rejection. Transplantation proceedings; 2006: Elsevier.
93. Schäffer M, Schier R, Napirei M, Michalski S, Traska T, Viebahn R. Sirolimus impairs wound healing. Langenbeck's archives of surgery. 2007;392:297-303.
94. Kang D-H, Kim Y-G, Andoh TF, Gordon KL, Suga S-I, Mazzali M, Jefferson JA, Hughes J, Bennett W, Schreiner GF. Post-cyclosporine-mediated hypertension and nephropathy: amelioration by vascular endothelial growth factor. American Journal of Physiology-Renal Physiology. 2001;280:F727-F36.
95. Basu A, Contreras AG, Datta D, Flynn E, Zeng L, Cohen HT, Briscoe DM, Pal S. Overexpression of vascular endothelial growth factor and the development of post-transplantation cancer. Cancer research. 2008;68:5689-98.
96. Guba M, Graeb C, Jauch K-W, Geissler EK. Pro-and anti-cancer effects of immunosuppressive agents used in organ transplantation. Transplantation. 2004;77:1777-82.
97. Campistol JM, Eris J, Oberbauer R, Friend P, Hutchison B, Morales JM, Claesson K, Stallone G, Russ G, Rostaing L. Sirolimus therapy after early cyclosporine withdrawal reduces the risk for cancer in adult renal transplantation. Journal of the American Society of Nephrology. 2006;17:581-9.
98. Alla SA, Quitterer U, Grigoriev S, Maidhof A, Haasemann M, Jarnagin K, Müller-Esterl W. Extracellular domains of the bradykinin B2 receptor involved in ligand binding and agonist sensing defined by anti-peptide antibodies. Journal of Biological Chemistry. 1996;271:1748-55.

Statutory Declaration

“I, Lei Chen by personally signing this document in lieu of an oath, hereby affirm that I prepared the submitted dissertation on the topic Funktionelle Charakterisierung der endothelvermittelten autoimmunen PAR-2 Aktivierung / Functional characterization of endothelial autoimmune PAR-2 activation, independently and without the support of third parties, and that I used no other sources and aids than those stated.

All parts which are based on the publications or presentations of other authors, either in letter or in spirit, are specified as such in accordance with the citing guidelines. The sections on methodology (in particular regarding practical work, laboratory regulations, statistical processing) and results (in particular regarding figures, charts and tables) are exclusively my responsibility.

My contributions to any publications to this dissertation correspond to those stated in the below joint declaration made together with the supervisor. All publications created within the scope of the dissertation comply with the guidelines of the ICMJE (International Committee of Medical Journal Editors; www.icmje.org) on authorship. In addition, I declare that I am aware of the regulations of Charité – Universitätsmedizin Berlin on ensuring good scientific practice and that I commit to comply with these regulations.

The significance of this statutory declaration and the consequences of a false statutory declaration under criminal law (Sections 156, 161 of the German Criminal Code) are known to me.”

Date Signature

Curriculum Vitae

My curriculum vitae does not appear in the electronic version of my paper for reasons of data protection.

Publications

Lei Chen had the following share in the following publications

[1] Du J, **Chen L**, Zhong C, Cheng C, Zhu X, Li R. Prediction and identification of linear B-cells epitope of human coagulant factor IX. Journal of Anhui Normal University(Natural Science Edition). 2014;37:569-74. (Chinsese)

[2] Du W, **Chen L**, Zhang L, Li R. Design and immunogenicity of B-cell epitope vaccine against human interleukin 6. Journal of University of Jinan (Science & Technology). 2015;29:34-8. (Chinsese)

[3] **Chen L**, Zhong C, Lin Z, Cheng C, Zhang L, Li R. A primary study of dextran-spermine conjugate as CpG ODN delivery vector. Genomics and Applied Biology. 2016;7:1738-42. (Chinsese)

[4] Zhong C, Zhang L, **Chen L**, Deng L, Li R. Coagulation factor XI vaccination: an alternative strategy to prevent thrombosis. Journal of Thrombosis and Haemostasis. 2017;15:122-30

[5] Catar R, Witowski J, Zhu N, Lücht C, Soria AD, Fernandez JU, **Chen L**, Jones SA, Fielding CA, Rudolf A, Topley N, Dragun D, Jörres A. IL-6 Trans–Signaling Links Inflammation with Angiogenesis in the Peritoneal Membrane. Journal of the American Society of Nephrology. 2017;28:1188-99.

[6] Zickler D, Luecht C, Willy K, **Chen L**, Witowski J, Girndt M, Fiedler R, Storr M, Kamhieh-Milz J, Schoon J, Geissler S, Ringdén O, Schindler R, Moll G, Dragun D, Catar R. Tumour necrosis factor-alpha in uraemic serum promotes osteoblastic transition and calcification of vascular smooth muscle cells via extracellular signal-regulated kinases and activator protein 1/c-FOS-mediated induction of interleukin 6 expression. Nephrology Dialysis Transplantation. 2017;33:574-85.

[7] Catar R, **Chen L**, Cuff SM, Kift-Morgan A, Eberl M, Kamhieh-Milz J, Zickler D, Parekh G, Davis P, Fraser D, Dragun D, Echkardt KU, Jörres A, Witowski J. Control of neutrophil influx during peritonitis by transcriptional cross-regulation of chemokine CXCL1 by IL-17 and IFN-γ (in submission to Journal of Pathology)

Acknowledgement

In the beginning, I would say thanks to my supervisor, Prof. Duska Dragun, for accepting me as her student, so that I have the chance to study in Charite, and to work with so many outstanding scientific researchers in the group. I have had a great time during the four years studying here!

Apart from my supervisor, I won't forget to express my sincere gratitude to Dr. Rusan Ali Catar for his continuous support of my doctoral study and related research work. His guidance helped me a lot in all the time of research and writing of this thesis. Without his patience, motivation, and immense knowledge, this work cannot be finished. Moreover, he taught me a variety of experimental techniques that will be useful for me in my future career. It will be hard for me to forget his guidance throughout my life!

I would also like to thank Aurelie and Angelika for the valuable suggestion for my thesis, and Dennis and Marc for their help and concerns. I would always remember my fellow labmates, Sumin Wu, Ola, Peng Ren and Qing Li for the companionship, help and the fun-time we spent together.

In the end, I am grateful to my parents for their 100% support and understanding to me no matter what decision I make. Encouragement, motivation and financial support from them give me the power to achieve my objective along the way.

In the past 4 years, I have got too much help from my colleagues, parent and relatives. I just want to wish them all, those who care about me, happy every day! Thank you!